YIELD STRESS STUDIES ON MOLTEN CHOCOLATE

by

Laurie L. Wilson

B. Sc. (Biology) University of British Columbia, 1984

A THESIS SUBMITTED IN PARTIAL FULFILLMENT OF

THE REQUIREMENTS FOR THE DEGREE OF

MASTER OF SCIENCE

in

THE FACULTY OF GRADUATE STUDIES

DEPARTMENT OF FOOD SCIENCE

We accept this thesis as conforming

to the required standard

THE UNIVERSITY OF BRITISH COLUMBIA

August 1991

In presenting this thesis in partial fulfilment of the requirements for an advanced degree at the University of British Columbia, I agree that the Library shall make it freely available for reference and study. I further agree that permission for extensive copying of this thesis for scholarly purposes may be granted by the head of my department or by his or her representatives. It is understood that copying or publication of this thesis for financial gain shall not be allowed without my written permission.

Department of Food Science

The University of British Columbia
Vancouver, Canada

Date August, 1991

ABSTRACT

A study of the flow properties of four chocolate samples was conducted. These were commercial semi-sweet (HSS), milk chocolate (HMC) and two experimental samples (H1 and H2). The yield stress, an important quality indicator of the chocolate, was estimated from steady shearing flow data by extrapolating the Casson model equation to zero flow rate and, by allowing stresses to relax after shearing. As well, undisturbed samples were examined in start-up flow using Single Vane and Multiple Vane methods. Proximate and sucrose analyses were carried out to determine the chemical composition of each chocolate sample. The mean particle size and the distribution of sizes contained in the samples was determined to further characterize the chocolates.

A multivariate analysis of variance indicated that there was a significant difference in chemical composition among the four test samples. The mean particle sizes ranged from 5.73 to 6.27, 6.98 and 7.15 μm for samples HSS, H1, HMC and H2, respectively. The greatest number of particles were in the size range of 4.0 to 5.0 μm.

The Casson model equation was fitted to steady flow data obtained with coaxial cylinder fixtures using a Brookfield HAT viscometer, a Brabender Rheotron viscometer, and a Carri-Med Controlled Stress Rheometer. For the Brookfield viscometer, the Casson equation over the shear rate range used, was found to accurately describe the flow characteristics of chocolate samples HMC, HSS and H2, but not sample H1.

For the Brabender viscometer and the Carri-Med rheometer, the Casson equation did not fit the flow data over the entire shear rate range used with each instrument. A deviation in linearity occurred below approximately 0.5 s^{-1} in the flow data measured in both instruments, thereby making the yield stress determination somewhat ambiguous.

Yield values recalculated using only the linear data points were higher. In addition, for the Brabender viscometer, significant differences ($p<0.05$) were observed in both the yield and viscosity values measured using two coaxial cylinder fixtures of different annular gap widths. Using the Carri-Med rheometer, a significant difference in viscosity ($p<0.05$) over consecutive test runs was found and a significant difference ($p<0.01$) in yield stress when samples were sheared for 12 minutes as compared to 30 minutes.

Yield stress estimates obtained using Multiple Vane Method I and Method II were comparable for chocolate samples HMC, HSS, and H2, but were significantly higher for sample H1 when using Method II as compared to Method I. Method II may be a more accurate estimate of the yield value of molten chocolate because the assumption of a uniform shear stress distribution over the ends of the vane fixture could not be proven experimentally for samples HSS and H1 when using Method I. Also, the dependence of the yield value on the rotational speed was evident when the vane data were analyzed using Method I, but was not a significant factor ($p>0.05$) when Method II was used to estimate yield stress. In addition, the single point measurements used to estimate yield stress agreed more closely with values obtained using Method II as compared to Method I.

It is postulated that the Single Vane Method or Multiple Vane Method II may provide more accurate estimates of the yield stress of molten chocolate than using the Casson approximation. For the vane methods, direct measurements were taken under virtually static conditions; whereas, in the Casson extrapolation method, yield stress was estimated indirectly from flow data over a broad shear rate range at stresses well beyond the yield point of the sample. The Single Vane Method was simple and required less time than fitting the Casson flow model to shear stress-shear rate data and, therefore, may be more suitable for routine yield stress measurements of molten chocolate in quality control laboratories.

TABLE OF CONTENTS

ABSTRACT ii

LIST OF TABLES vii

LIST OF FIGURES xi

NOMENCLATURE xiii

ACKNOWLEDGEMENT xiv

1 INTRODUCTION 1

2 LITERATURE REVIEW 4

2.1 RHEOLOGICAL PROPERTIES OF MOLTEN CHOCOLATE 4

2.1.1 Factors Influencing Flow Properties 4

2.1.2 Historical Background 6

2.2 FUNDAMENTALS OF ROTATIONAL VISCOMETRY 10

2.3 RHEOMETER DESCRIPTION 11

2.3.1 Brookfield Viscometer 11

2.3.2 Brabender Rheotron Viscometer 12

2.3.3 Carri-Med Controlled Stress Rheometer 12

2.4 STRESS RELAXATION METHOD 15

2.5 VANE FIXTURE METHOD 18

2.5.1 Theory 18

2.5.1 Theory 18

3 EXPERIMENTAL **22**

3.1 CHOCOLATE SAMPLES 22

3.1.1 Product Description 22

3.2 CHEMICAL ANALYSES 22

3.2.1 Moisture 23

3.2.2 Ash 23

3.2.3 Crude Protein 23

3.2.4 Fat 24

3.2.5 Sucrose 25

3.3 PARTICLE SIZE ANALYSIS 26

3.4 YIELD STRESS DETERMINATION 26

3.4.1 Calibration 26

3.4.2 Sample Preparation 27

3.4.3 Indirect Methods 29

3.4.4 Direct Methods 31

3.5 DATA ANALYSES 34

4 RESULTS AND DISCUSSION **35**

4.1 CHEMICAL ANALYSES 35

4.2 PARTICLE SIZE ANALYSIS 37

4.3 INDIRECT ESTIMATION OF YIELD STRESS 41

4.3.1 Brookfield Viscometer 41

4.3.2 Brabender Rheotron Viscometer 44

4.3.3 Carri-Med Controlled Stress Rheometer 50

4.4 STRESS RELAXATION METHOD 57

4.5.1 Single Vane Method 59
4.5.2 Multiple Vane Method I 66
4.5.3 Multiple Vane Method II 70

5 CONCLUSIONS 75

LITERATURE CITED 79

APPENDIX 86

A LISTING OF EXPERIMENTAL FLOW DATA 86

LIST OF TABLES

3.1 Instrument parameters for the coaxial cylinder fixtures used. 28

3.2 Vane fixture dimensions 33

4.3 Composition of the chocolate samples. 36

4.4 Multivariate analysis of variance for chemical composition. 38

4.5 Range and mean sizes of particles in the chocolate samples. 39

4.6 Casson flow parameters for chocolate melts at 40°C obtained with the Brookfield HAT viscometer using the SC4-27/13R bob and cup fixture. . 43

4.7 Casson flow parameters for chocolate melts at 40°C obtained with the Brabender Rheotron using coaxial cylinder fixtures A1 and A2. 45

4.8 Analysis of variance for Casson yield stress obtained with the Brabender Rheotron using coaxial cylinder fixtures A1 and A2. 46

4.9 Analysis of variance for viscosity obtained with the Brabender Rheotron using coaxial cylinder fixtures A1 and A2. 46

4.10 Casson yield stress estimates for chocolate samples at 40°C recalculated over the linear portion of the rheograms obtained with the Brabender Rheotron using coaxial cylinder fixtures A1 and A2. 47

4.11 Casson flow parameters for chocolate samples at 40°C obtained with the Carri-Med rheometer using coaxial cylinder fixture 5222. 51

4.12 Analysis of variance for Casson yield stress of chocolate samples at 40°C over consecutive runs obtained with the Carri-Med rheometer using coaxial cylinder fixture 5222. 52

4.13 Analysis of variance for Casson viscosity of chocolate samples at 40°C over consecutive runs obtained with Carri-Med rheometer using coaxial cylinder fixture 5222. 52
4.14 Mean Casson yield stress estimates for chocolate samples at 40°C recalculated over the linear portion of the rheograms obtained with the Carri--Med rheometer using coaxial cylinder fixt ure 5222. 55
4.15 Casson yield stress estimates for chocolate samples H1 and H2 at 40°C for two run times obtained with the Carri-Med rheometer using coaxial cylinder fixture 5222. 56
4.16 Analysis of variance for Casson yield stress of chocolate samples at 40°C for two run times obtained with the Carri-Med rheometer using coaxial cylinder fixture 5222. 56
4.17 Yield stress estimates for chocolate samples at 40°C using the Stress Relaxation Method and the Brabender viscometer with coaxial cylinder fixtures A1 and A2. 58
4.18 Yield stress estimates for chocolate samples at 40°C using the Single Vane Method. 60
4.19 Split plot analysis of variance for estimates of yield stress in chocolate samples at 40°C using the Single Vane Method. 62
4.20 Yield stress estimates for chocolate samples at 40° C from extrapolating mean yield stress values for vanes at three start-up speeds to zero rpm. . . 63
4.21 Yield stress estimates for chocolate samples at 40°C using Method I for analyzing vane fixture data. 67
4.22 Analysis of variance in yield stress estimates derived at various rotational speeds in chocolate samples at 40°C using multiple vane fixture data analyzed by Method I. 69

4.23 Yield stress estimates for chocolate samples at 40°C using Method II for analyzing vane fixture data. 71

4.24 Analysis of variance for yield stress estimates derived at various rotational speeds for chocolate samples at 40°C using multiple vane fixture data analyzed by Method II. 73

A.25 Shear stress data (Pa) for chocolate samples at 40°C obtained with the Brookfield HAT Viscometer using coaxial cylinder fixture SC4-27/13R for steady shear tests at ascending (asc) and descending (dsc) shear rate. . . 87

A.26 Shear stress data (Pa) for chocolate samples at 40°C obtained with the Brabender Rheotron viscometer using coaxial cylinder fixture A1 and spr ing C for steady shear tests at ascending (asc) and descending (dsc) shear rate. 88

A.27 Shear stress data (Pa) for chocolate samples at 40°C obtained with the Brabender Rheotron viscometer using coaxial cylinder fixture A2 and spr ing C for steady shear tests at ascending (asc) and descending (dsc) shear rate. 89

A.28 Shear rate data (s^{-1}) for chocolate samples at 40°C obtained with the Carri-Med rheometer and coaxial cylinder fixture 5222 for controlled stress tests at ascending (asc) and descending (dsc) shear stress. 90

A.29 Shear rate data (s^{-1}) for chocolate sample H1 at 40°C obtained with the Carri-Med rheometer and coaxial cylinder fixture 5222 for controlled stress tests at ascending (asc) and descending (dsc) shear stress for 12 and 30 minute run times. 96

A.30 Shear rate data (s^{-1}) for chocolate sample H2 at 40°C obtained with the Carri-Med rheometer and coaxial cylinder fixture 5222 for controlled stress tests at ascending (asc) and descending (dsc) shear stress for 12 and 30 minute run times. 102

A.31 Peak torque values for chocolate samples at 40°C using different sized vanes with the Brabender Rheotron viscometer with the A cup and spring A. 108

LIST OF FIGURES

2.1 Model rheograms for Newtonian (1), Bingham (2) and Casson (3) flow behavior. 11

2.2 Schematic diagram of the Brookfield SC4-27/13R coaxial cylinder fixture and water jacket assembly (to scale). 13

2.3 Schematic diagram of the Brabender coaxial cylinder fixture A1 (bob diameter is 54.0 mm, height is 80.0 mm and cup diameter is 56.0 mm) and water jacket (to scale). 14

2.4 Schematic diagram of the Carri-Med coaxial cylinder fixture, (bob diameter is 37.0 mm, height is 50.0 mm, and cup diameter is 41.5 mm), water jacket and Peltier plate (to scale). 16

2.5 Diagram of a vane fixture used to measure yield stress. The vane shown has a blade height of 40.0 mm, and four blades of diameter 25.0 mm (to scale). 21

4.6 Distribution of sizes for particles contained in the chocolate samples . . . 40

4.7 Casson flow curves of chocolate samples at 40°C obtained with the Brookfield HAT Viscometer using the SC4-27/13R bob and cup fixture. 42

4.8 Casson flow curves of chocolate samples at 40°C obtained with the Brabender Rheotron viscometer using coaxial cylinder fixture A1. 48

4.9 Casson flow curves of chocolate samples at 40°C obtained with the Brabender Rheotron viscometer using coaxial cylinder fixture A2. 49

4.10 Casson flow curves of chocolate samples at 40°C obtained with the Carri-Med rheometer using coaxial cylinder fixture 5222. 54
4.11 Yield stress estimated at zero rpm for the chocolate samples at 40°C using mean yield values obtained from the five vane fixtures. 65
4.12 Plot of $2T_m/\pi D^3$ versus H/D (Method I) for estimating yield stress of chocolate samples at 40°C using vane fixtures E, F, G, K and O. 68
4.13 Plot of peak torque versus vane height (Method II) for estimating yield stress of chocolate samples at 40°C using vane fixtures G, K and O. . . . 72

NOMENCLATURE

a	Ratio of bob radius to cup radius, r_b/r_c.
D	Diameter of vane fixture.
h	Height of bob fixture.
H	Height of vane fixture.
M	Torque (coaxial cylinder fixture) (N·m).
p	Probability level for testing statistical significances.
rpm	Revolutions per minute.
r^2	Coefficient of determination.
r_b	Bob radius.
r_c	Cup radius.
T	Torque (vane fixture) (N·m).
T_m	Peak torque or maximum on start-up (N·m).
η	Apparent viscosity ($Pa \cdot s^{-1}$).
η_{ca}	Casson viscosity ($Pa \cdot s^{-1}$).
η_p	Bingham plastic viscosity ($Pa \cdot s^{-1}$).
$\dot{\gamma}$	Shear rate (s^{-1}).
$\dot{\gamma}_N$	Newtonian shear rate (s^{-1}).
Ω	Angular velocity ($rad \cdot s^{-1}$).
π	pi.
σ	Shear stress (Pa).
σ_{ca}	Casson shear stress (Pa).
σ_y	Yield stress (Pa).

ACKNOWLEDGEMENT

The author wishes to express her sincere appreciation to Dr. Marvin A. Tung for his patience, advice and review of this thesis. She also wishes to thank the members of her research committee: Dr. William D. Powrie, Dr. John Vanderstoep and Dr. Timothy D. Durance for their constructive criticism and review of this thesis.

Special thanks are extended to Ian Britt, Gerry Morello, Steve Owen, Agnes Papke and Dr. Alex Speers. She is especially grateful to her husband, Damir Cukor, for his patience, support and encouragement.

Financial support was provided in part by the Natural Sciences and Engineering Research Council of Canada. The experimental chocolate samples were kindly donated by Hershey Chocolate Company.

Chapter 1

INTRODUCTION

The yield stress is defined as the point at which a plastic substance begins to flow under an applied shear stress (Keentok, 1982). Many food products such as applesauce, mayonnaise, ketchup and molten chocolate exhibit non-Newtonian fluid behavior and possess a yield stress (Barbosa-Canovas and Peleg, 1983; Tiu and Boger 1974). Accurate measurement of the rheological properties and, in particular, the yield stress is important for process design and control, as well as for predicting product performance and sensory quality (Dervisogul and Kokini, 1986).

Measuring the yield stress is not a simple task. There exists in the literature a variety of methods to chose from and the use of different methods can result in yield values that differ significantly. Other complicating factors may include time dependency, shear history, sample handling, temperature effects and the type of rheometer used (De Kee et al., 1983; Prentice and Huber, 1983; Paredes et al., 1989).

Rotational viscometers remain the most widely used instruments for the measurement of flow properties of fluid-like materials today (Levine, 1987). The most common method of measuring yield stress is to measure steady shearing flow in a rotational instrument and extrapolate the shear stress-shear rate data to a zero rate of shear in order to obtain the yield value (Charm, 1963; Vocadlo and Charles, 1971; Nguyen and Boger, 1983). Usually one or more constitutive equations may be fitted to the flow data to form a linear relationship which may then be extrapolated to obtain an estimate of yield stress. Common rheological models used include the Bingham, Power-law, Herschel-Bulkley and

Casson models.

The Casson model has been accepted as the official method used to describe the flow of molten chocolate (OICC, 1973). Although it has been reported that this equation does not fit the flow data over the entire shear rate range used, this method is commonly used in quality control and in research to estimate the yield stress of molten chocolate (Prentice and Huber, 1981; Sequine, 1986). Deviation from linearity below 5 s^{-1} has been reported and it is recommended that the chocolate melt be tested within the range of 5 to 60 s^{-1} (Steiner, 1962; OICC, 1973). However, it is in the low shear rate range that yielding to an applied stress (or strain) occurs and one could argue that this is where measurements should be made to estimate yield values.

Modifications made to the Casson equation have brought only limited success (Heimann and Fincke, 1962c; Saunders, 1968). Furthermore, this equation, which was developed to characterize the flow of printing ink suspensions, was based on the theory of agglomeration and disagglomeration of particles during flow which may not be true for molten chocolate (Niediek, 1980). Other flow equations proposed include constants that relate to some physical properties of the chocolate, but no further research using these equations has been carried out (Charm, 1963; Sommer, 1974).

An alternative approach would be to use direct methods of yield stress measurement. One technique in which the residual stress after shearing is measured, uses the equilibrium stress value at rest as an estimate of the yield stress value of the sample. As well, a method using vane fixtures, which has been used to estimate the yield values of clay suspensions (Nguyen and Boger, 1983), could be applied to molten chocolate. In this method, yield stress can be estimated from torque readings at the onset of vane rotation from a resting state.

The objectives of the present research were:

1. To study the application of the Casson flow model for the determination of the yield stress value of molten chocolate from steady shear and controlled stress flow data.

2. To assess the validity of a stress relaxation and vane fixture methodology for the direct determination of the yield stress value of molten chocolate.

Chapter 2

LITERATURE REVIEW

2.1 RHEOLOGICAL PROPERTIES OF MOLTEN CHOCOLATE

Molten chocolate, like many food products, displays non-Newtonian fluid-like behavior and is characterized by the presence of a yield stress (Charm, 1963). When subjected to slowly increasing stresses below the yield point, the chocolate behaves like an elastic solid, deforming in proportion to the applied stress, until the yield stress is exceeded. At higher stresses, the melt flows as a viscous fluid. From a rheological standpoint, materials that have a yield stress but can be made to flow at higher stresses are said to have plastic properties. Chocolate in the melted state is pseudoplastic or shear rate thinning which is a reversible effect in which the the resistance to flow (apparent viscosity) decreases with increasing shear rates (Motz, 1964; Malm, 1968; Kleinert, 1976). This thinning effect is more apparent in low fat chocolates (Chevalley, 1975).

2.1.1 Factors Influencing Flow Properties

Molten chocolate is essentially a suspension of finely ground solid particles in a continuous liquid fat phase (Rostagno, 1974). The flow properties of this suspension are influenced by chemical composition, temperature, particle size and solids content (Chevalley, 1975; Kleinert, 1976). In particular, yield stress is thought to be due to interactions between suspended particles that form a kind of structure (Davis et al., 1968; Hunter and Nicol, 1968; Kleinert, 1976; Wildemuth and Williams, 1985).

Chocolate is a particularly complex food, consisting of fats, proteins, carbohydrates, minerals, cellulose and water. Simple model systems of cocoa powder and fat, with added sugar and/or emulsifier, and specifically formulated chocolates, have provided some insight into which components influence flow (Rostagno et al., 1974; Kleinert, 1976). Cocoa particles are hydrophobic and interact with the fat phase, whereas the sugar crystals are hydrophilic (Tscheuschner and Markov, 1986). The presence of milk protein and the type of milk protein used would further affect the nature of the interactions occurring between particles in the chocolate melt (Heathcock, 1985). When lecithin, an emulsifier, is added at very low concentrations of 0.1 to 0.5%, it acts primarily as a surface active agent reducing the friction between the sugar, protein and cocoa particles, during the conching process, and causes a reduction in both yield stress and viscosity (Kleinert, 1976; Tscheuschner and Wünsche, 1979).

Increasing the fat content will also cause a decrease in measured yield and viscosity values (Chevalley, 1975). Increasing the solids content and/or decreasing the particle size during refining will, not surprisingly, increase the viscosity and yield values (Malm, 1967b; Kuster, 1985). Molten chocolate is usually tested at a temperature of 40°C and a variation of 1°C at this temperature will result in a 2-3% change in viscosity and a 0.5-1% change in yield stress. When temperature is increased over the range of 40 to 60°C, the viscosity decreases and the yield stress increases dramatically (Heimann and Fincke, 1962d; Rostagno, 1974).

In the solid form, chocolate is a relatively stable food product when stored at temperatures between 18 and 20°C. Higher or lower temperature fluctuations over a period of months may adversely effect the texture and appearance of the chocolate. As well, chocolate and compound chocolates are best stored at a relative humidity ranging from 50 to 70%. Chocolates will absorb moisture if the relative humidity is above 78% for milk chocolate and above 82 to 85% for dark chocolates (Minifie, 1980; Abbink, 1984;

Cockinos, 1985; Reade, 1985).

For practical applications, the rheological behavior of chocolate and the factors which influence flow are of the utmost importance when sizing pipes and designing pumps, and when using the chocolate for molding or coating. Therefore, an accurate description of flow and, in particular, the yield phenomenon, is necessary for process and product control.

2.1.2 Historical Background

Over thirty years ago, the Bingham model was used to describe the rheological behavior of molten chocolate. This model is represented by the following equation,

$$\sigma = \sigma_y + \eta_p \dot{\gamma} \tag{2.1}$$

where σ is the shear stress (Pa), σ_y is the yield stress (Pa), η_p is the the plastic viscosity (Pa· s^{-1}), and $\dot{\gamma}$ is the shear rate (s^{-1}). If the material is a true Bingham plastic, the shear stress-shear rate data will form a straight line on linear coordinates where the slope is the plastic viscosity and the intercept is the yield stress.

In studying the work of other researchers, Steiner (1958) concluded that the Bingham equation did not adequately describe the rheological behavior of molten chocolate. The flow curves were relatively linear over a shear rate range of 15 to 100 s^{-1}, but there was a pronounced curvature concave to the shear rate axis at shear rates under 15 s^{-1}. Using flow data over a wide range of shear rates with extrapolation to zero shear rate would result in an over-estimation of the yield value.

A slightly more complex two-parameter model was derived theoretically by Casson (1957) and tested by Bantoft (1957) on dispersions of pigments in castor oil (Steiner, 1958; Casson, 1959). A simplified form of this equation is written as,

$$\sqrt{\sigma} = \sqrt{\sigma_{ca}} + \sqrt{\eta_{ca}\dot{\gamma}} \tag{2.2}$$

where σ_{ca} is the Casson yield stress (Pa) and η_{ca} is the Casson infinite shear viscosity (Pa·s^{-1}). Steiner (1958; 1962) found this model fitted the chocolate melt flow data more accurately than did the Bingham model. He found that a linear relationship existed when the square root of shear stress was plotted against the square root of shear rate over a shear rate range of 1 to 100 s^{-1} when several types of chocolates were tested using different rotational viscometers.

The Casson flow model was first applied to oil suspension data using cone and plate fixtures with a rotational rheometer. In this type of sample fixture, the shearing volume or gap increases in thickness from the center of rotation out to the edge of the fixture in proportion to the increasing relative velocity between the cone and plate surfaces, therefore the rate of shear is constant throughout the volume of the sample. In coaxial cylinder fixtures, the annular gap between the cylinders would subject a Newtonian fluid to a shear rate which varies inversely with the square of the radial position. Therefore, the rate of shear for Newtonian fluids is not constant across the gap and the shear rate profile for non-Newtonian fluids is more complex. The Reiner-Riwlin equation corrects for non-Newtonian shear rates in Bingham materials (Van Wazer et al., 1963). An equivalent correction was calculated by Steiner (1958) and later by Hanks (1983). Although the mathematical approach differs among the three separate groups, the correction is essentially the same. Darby (1985) applied the power-law shear rate correction (Krieger, 1968) to the Bingham and Casson models and estimated the percentage error in shear rate to be approximately 6% for Casson materials in narrow gap coaxial cylinder fixtures.

Steiner's original equation for the exact relation between shear rate and shear stress for Casson flow is as follows:

$$\dot{\gamma} - 4\frac{\sigma_{ca}}{\eta_{ca}}\frac{(1-a)^2}{(1+a)^4}\left(\frac{1}{3}+\frac{1}{5}\left[\frac{1-a}{1+a}\right]^2+\ldots\right) = \frac{1}{\eta_{ca}}\left(\sqrt{\sigma}-\frac{2\sqrt{\sigma_{ca}}}{1+a}\right)^2 \qquad (2.3)$$

The value of a represents the ratio of bob radius to cup radius. The second term on the

left hand side of the equation may be ignored when the value of a is close to 1.0. (as in a narrow gap viscometer). Another condition stated that the ratio of σ_{ca}/η_{ca} must also not exceed 10 if the term is to be omitted. This ratio is usually between 5 and 8 for most chocolates (Steiner, 1958; Sequine, 1986). Therefore the numerical value of this term is still less than 1.0 even when a is 0.5 and the σ_{ca}/η_{ca} ratio is as high as 10. When these conditions are accounted for, the flow equation becomes:

$$(1+a)\sqrt{\dot{\gamma}} = \frac{1}{\sqrt{\eta_{ca}}}\left[(1+a)\sqrt{\sigma} - 2\sqrt{\sigma_{ca}}\right] \tag{2.4}$$

In order to evaluate the Casson flow properties, (1+a)$\sqrt{\sigma}$ may be plotted against (1+a)$\sqrt{\dot{\gamma}}$ to obtain a straight line which may be extrapolated to zero shear rate. The Casson infinite shear viscosity is calculated from the slope and the Casson yield stress from the intercept.

A modified Casson equation was suggested by Heimann and Fincke (1962a; b; c) as follows:

$$\sigma^{2/3} = \sigma_{ca}^{2/3} + (\eta_{ca}\dot{\gamma})^{2/3} \tag{2.5}$$

They stated that this model equation fitted flow data more accurately for many milk chocolates. Also, a more general flow equation was given,

$$\sigma^m = \sigma_y^m + (\eta\dot{\gamma})^m \tag{2.6}$$

where the exponent m was termed the flow index. Saunders (1968a) recommended that the optimum value of the flow index could be obtained by adjusting m by increments of 0.05 until the best fit to the flow data was achieved. He suggested that the value of m may be related to the structural characteristics of the chocolate and would not necessarily take on values of 0.5 or 2/3 as in the Casson or Heimann and Fincke models, respectively. However, in a collaborative study, values reported for the flow index, m, for samples tested, varied between laboratories (Steiner, 1972).

The original Casson equation provided good approximations of the flow properties of most chocolates, and was therefore considered when there was a need to standardize the methodology. The Casson model became the provisional method of the International Office of Cocoa and Chocolate (OICC) in 1960, remained as such in an Office publication in 1970, and then was later accepted in its final form in 1973. The OICC protocol is widely used in research and in the European chocolate manufacturing industry (Malm 1967a; 1968; Banford et al., 1970; Chevalley, 1975; Niediek, 1980; 1981).

In North America, the Casson model was slow to gain recognition over the years. Duck (1965) stated that the Casson parameters better defined the flow properties of chocolate as compared to using MacMichael viscosity which was the standard method of the American Association of Candy Technologists and the National Confectioners Association (Minifie, 1980). Duck detailed modifications made to a Brookfield viscometer and developed a nomograph for this instrument that would greatly simplify the determination for routine work. Howard (1969a; b) and Robbins (1979) outlined further changes made to the Brookfield HBT viscometer which could be used to measure both MacMichael viscosity and the Casson values. By 1986, a tentative methodology for the measurement of the Casson flow parameters was finalized by the National Confectioners Association (Sequine, 1986). The standard methodology is used mainly for quality control purposes and for research and development in the chocolate industry. Relatively little activity is evident in university or public sector laboratories, thus there is little published work on the flow properties of molten chocolate available in North America (Solstad, 1983; Zangger, 1984; Sequine, 1986).

Recent studies on chocolate have included the development of a thermo-rheometry process where the flow properties of *tempered* chocolate masses have been measured (Kleinert, 1982a; b; c). In addition, the texture characteristics of solid chocolate have been described in terms of instrument parameters and in sensory studies (Tscheuschner

and Markov, 1986; Markov and Tscheuschner, 1989).

2.2 FUNDAMENTALS OF ROTATIONAL VISCOMETRY

In classical rotational viscometry, a rotating body is immersed into a fluid and the viscous drag of the fluid exerting a opposing force is measured (Van Wazer et al., 1963). Rotational fixture designs include cone and plates, parallel plates and coaxial cylinders. For the coaxial cylinder fixture acting upon a Newtonian liquid, the shear rate is proportional to the rotational speed of the bob (or cup) and can be calculated from the dimensions of the fixture using the following equation(s):

$$\begin{aligned} \dot{\gamma}_N &= 2\Omega \left[\frac{r_c^2}{r_c^2 - r_b^2} \right] \\ &= \frac{4\pi\, rpm}{60} \left[\frac{r_c^2}{r_c^2 - r_b^2} \right] \end{aligned} \tag{2.7}$$

where $\dot{\gamma}_N$ is the Newtonian shear rate, Ω is the angular velocity and r_c and r_b are the radius of the cup and bob, respectively. However, the assumption of Newtonian flow for non-Newtonian fluids can lead to appreciable error in calculated shear rates and should be corrected for. Shear stress can be calculated from the measured torque and the fixture dimensions as follows:

$$\sigma = \frac{M}{2\pi r_b^2 h} \tag{2.8}$$

where M is the torque, r_b is the radius of the bob, and h is the height of the bob.

Flow graphs may be constructed from the shear stress-shear rate data in order to assess the flow behavior of the material (Figure 1.1). An ideal Newtonian (viscous) fluid is shown in curve 1. A Bingham plastic (curve 2) behaves as a solid until stressed beyond its yield value where a further increase in shear rate shows a proportional increase in shear stress. For a Casson material, after the yield point has been reached, the flow is nonlinear as shown in curve 3.

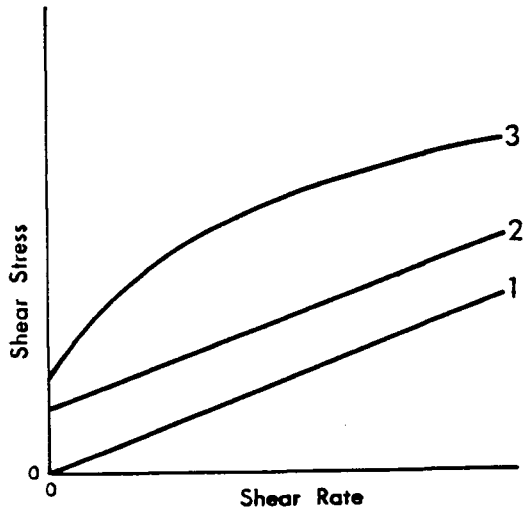

Figure 2.1: Model rheograms for Newtonian (1), Bingham (2) and Casson (3) flow behavior.

2.3 RHEOMETER DESCRIPTION

2.3.1 Brookfield Viscometer

Brookfield viscometers are well known and have been widely used for viscosity measurement in industry for over forty-five years. This viscometer is relatively inexpensive, reliable and easy to use. As well, the availability of a wide variety of sample fixtures such as the small sample adapter and a narrower gap cup and bob geometry (UL fixtures), as well as cone and plate fixtures, make this instrument comparable to more expensive rheometers (Rosen and Foster, 1978; Smith, 1982; Brownsey, 1988). A synchronous induction-type motor transmits power through a gear drive assembly producing either four or eight specific rotational speeds, depending on the model. The HAT model, used in this investigation, has eight possible speeds and is recommended for high viscosity materials like molten chocolate (Brookfield, 1985). The SC4-27/13R stainless steel bob and cup fixture is generally used along with a water jacketed small sample adapter allowing

for thermostatic control (Figure 2.2).

The torque required to maintain a constant angular velocity of the immersed bob in the sample is measured via a calibrated spring which has been preset at the factory (Sequine, 1986). The bob has conical ends which helps to minimize error due to shear stresses occuring on the bottom and top of the bob (Howard, 1969; Powell, 1988).

2.3.2 Brabender Rheotron Viscometer

The Brabender Rheotron viscometer has a much broader capability than the Brookfield viscometer. It can be used with both coaxial cylinder and cone and plate fixtures which are suitable for testing a variety of materials over a broad shear rate range (0.05 to 20,000 s^{-1}). There are 32 discrete operating speeds. Accurate speed control is accomplished through a d.c. servo-motor which is coupled, by magnetic clutches, to the gear box.

The outer cylinder is rotated while the torque is measured at the bob (Figure 2.3). The torque measuring sensor features 3 interchangeable springs extending the shear stress range from approximately 0.25 to 10^5 Pa. This instrument can also be used with an optional speed programmer allowing for continuous shear in a linearly increasing and/or decreasing manner.

2.3.3 Carri-Med Controlled Stress Rheometer

The first controlled stress rheometer was developed in the late 1960's by Davis, Deer and Warburton at the London School of Pharmacy (Davis et al., 1968). This prototype was later marketed as the Deer Variable Stress Rheometer which originally used turbines to support and apply a constant stress to the inner rotating cylinder of the coaxial cylinder fixture. Later, an induction drive motor replaced the air turbine.

The Carri-Med controlled stress rheometer, in which Deer had been involved, is referred to as a third generation instrument. It has a microprocessor-controlled induction

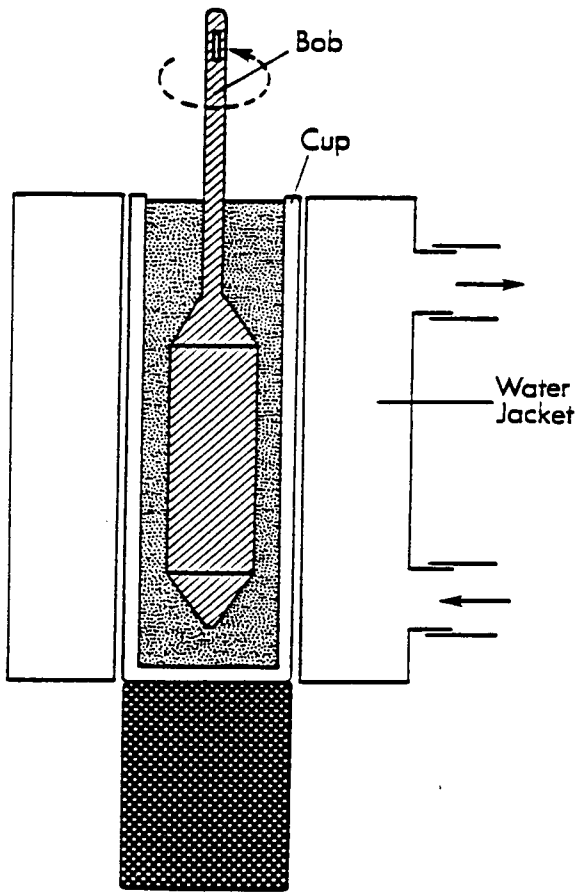

Figure 2.2: Schematic diagram of the Brookfield SC4-27/13R coaxial cylinder fixture and water jacket assembly (to scale).

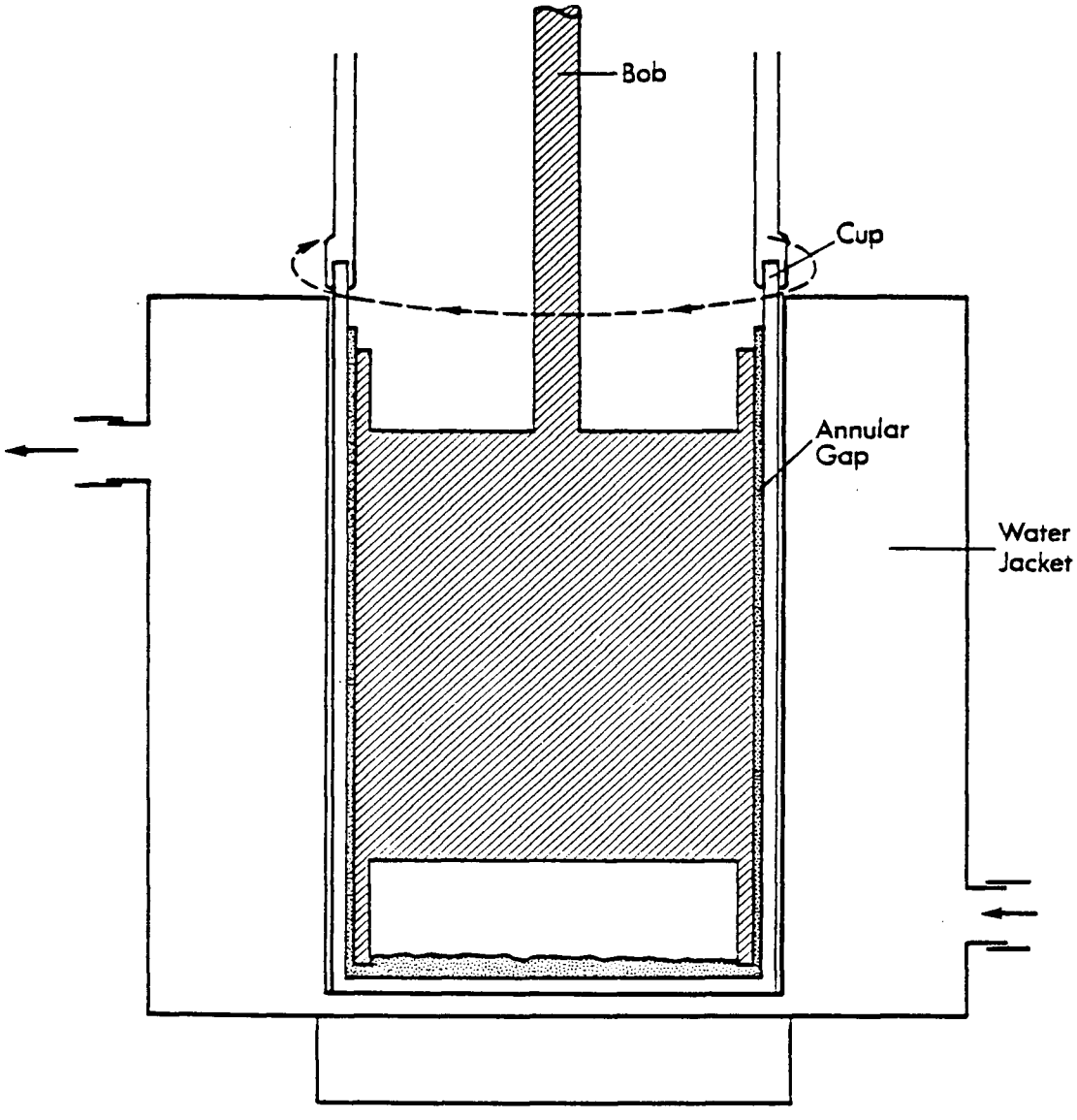

Figure 2.3: Schematic diagram of the Brabender coaxial cylinder fixture A1 (bob diameter is 54.0 mm, height is 80.0 mm and cup diameter is 56.0 mm) and water jacket (to scale).

drive motor system and can be used for a broad array of rheological tests. Although this instrument can be used manually, control through a microcomputer (either Apple or IBM) not only directs the machine but provides data logging and software for flow analysis using the Casson, Bingham, Herschel-Bulkley and other models (Brownsey, 1988).

Controlled stress rheometers differ from conventional controlled shear rate rheometers in two important ways. Firstly, in controlled stress testing, the sample may be sheared over a broader range continuously without having to change the torque measuring device, or gear ratio, in order to increase or decrease speed. Secondly, the behavior and deformation of the sample at very low stresses can be studied (Cheng, 1986; Carri-Med, 1985).

The Carri-Med narrow gap coaxial cylinder fixture, used in this investigation, is shown in Figure 2.4. This fixture is comparable to the one shown for the Brabender in that it features a hollow cavity in the bottom of the inner cylinder which traps a volume of air to help eliminate viscous drag by contact of the sample with the base of the bob. Standard equations for the calculation of shear stress and shear rate remain the same.

Being a relatively new instrument, full use of the rheometer was limited by delays in developing comprehensive computer control and data analysis capablities (Brownsey, 1988). However, because controlled stress rheometers have now become so highly automated, versatile and relatively straight forward to use, applied stress testing is being used more extensively in research today (Franck, 1985; Yoshimura et al., 1987; Barnes and Carnali, 1990).

2.4 STRESS RELAXATION METHOD

Stress relaxation techniques have been used to determine the yield stress of a variety of food and non-food materials. This is a simple method and involves shearing the sample

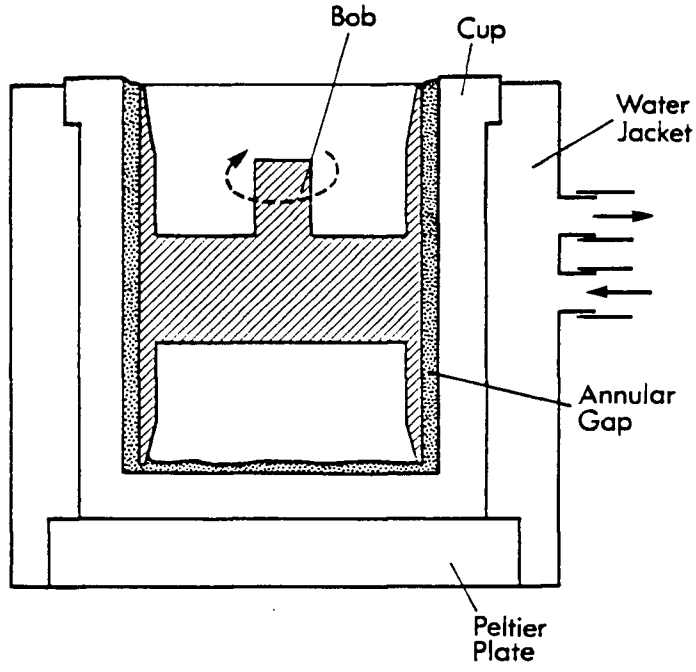

Figure 2.4: Schematic diagram of the Carri-Med coaxial cylinder fixture, (bob diameter is 37.0 mm, height is 50.0 mm, and cup diameter is 41.5 mm), water jacket and Peltier plate (to scale).

at a low steady shear, then reducing the speed either gradually or suddenly and recording the decline in shear stress to an equilibrium value as a function of time (Michaels and Bolger, 1962; Tiu and Boger, 1974; Nguyen and Boger, 1983). Different test fixtures such as the parallel plate, bob and cup and cone and plate geometries have been used to measure residual stress (Patton, 1966; Tiu and Boger, 1974; Keentok, 1982). The equilibrium stress value can be graphically determined as described by Patton (1966) and the raw data converted to obtain plots of viscosity versus shear rate, or, shear stress versus shear rate. The shear stress-shear rate data can also be used to extrapolate to zero shear rate to estimate yield stress (Swartzel et al., 1980).

Reproducibility of the stress relaxation method can sometimes be a problem. For greases (Keentok, 1982) and concentrated suspensions (Vocadlo and Charles, 1971; Nguyen and Boger,1983), slip between the sample and fixture surfaces can occur, thereby resulting in inaccurate yield stress estimates. If long relaxation times are required, dense particles in the sample can settle out (Nguyen and Boger, 1983). Using fixtures made of different materials (Vocadlo and Charles, 1971) or different fixture geometries (Keentok, 1982) can result in significantly different yield stress values.

As well, it can be difficult to distinguish between the effects of shear-thinning and time dependency (Smith, 1982). For example, residual stress measurements for mayonnaise were found to depend on the time of shear (Tiu and Boger, 1974). It is important, therefore, to repeat the relaxation test under several conditions. The use of different shear rates and shearing times has been recommended, before measuring the equilibrium stress after relaxation. (Barbosa-Canovas and Peleg, 1983; Nguyen and Boger, 1983). While stress relaxation may be inappropriate for some materials it has been used successfully for paints (Patton, 1966; Smith, 1982), guar gum and cornstarch dispersions (Lang and Rha, 1981), tomato puree and applesauce (Charm, 1963), and for moderately concentrated clay suspensions (Nguyen and Boger, 1983). Yield stress values were comparable to

those obtained using indirect extrapolation methods.

2.5 VANE FIXTURE METHOD

The use of constitutive equations like Casson's to arrive at a yield stress value are empirical and dependent on the model, the accuracy of the flow data and the type of rotational instrument used (Nguyen and Boger, 1983). Some research has been done using the vane fixture (Figure 2.5) as an alternative to the coaxial cylinder fixture in rotational viscometry.

In soil mechanics, a simple vane technique has been widely used for many years to measure the shear strength of cohesive soils. Over the past decade researchers have adopted the vane method to measure the yield stress of clay suspensions, emulsions and greases (Keentok, 1982; Nguyen and Boger, 1983; 1985; James et al., 1987; Yoshimura, 1987). In food rheology, research by Tung et al. (1990) in which this author is involved, has used vane fixtures to test mayonnaise, salad dressing and chocolate melts.

In recent studies, comparisons have been made between vane fixture methods and steady shearing flow extrapolation methods using flow models (Keentok, 1982; Nguyen and Boger 1983; Tung and Speers, 1986; James et al., 1987; Tung et al., 1990). It has been suggested that when testing highly concentrated dispersions, the vane fixture method could provide a more accurate yield stress measurement over the conventional coaxial cylinder fixture method where slip effects on the surface of the cylinder can introduce significant error.

2.5.1 Theory

The vane method employed with constant speed instruments involves immersing the vane fixture into a cup containing the sample and slowly rotating the vane at a constant

rotational speed while measuring the torque response as a function of time. As the vane rotates, the material deforms elastically, with the torque increasing to a maximum value before dropping off to a lower equilibrium value. The presence of a peak torque on a torque-time curve is characteristic of materials possessing a yield stress. The shape of the torque-time curves may also be influenced by the nature of the instrumentation used. For example, with viscometers that have the torsion transducer in the drive system between the motor and vane fixture, the transducer compliance, fixture and sample inertia, and recording system characteristics may play a role in determining the appearance of the resulting curves.

It has been demonstrated that the yielding of the material occurs along the cylindrical surface described by the rotating vane (as shown in Figure 2.5). The torque, T, is due to shearing of the sample on the cylindrical surface and two ends of the vane and is equal to:

$$T = \left(\frac{\pi}{2} D^2 H\right) \sigma_s + 2 \left(2\pi \int_0^{D/2} \sigma_e r^2 dr\right) \tag{2.9}$$

where D and H are the diameter and height of the vane respectively, σ_s is the shear stress on the cylindrical yielding surface and σ_e is the end shear stress which is unknown (Nguyen and Boger, 1985).

To calculate yield stress from measured torque, it is assumed that the end shear stress is constant and equal to the shear stress on the curved shearing surface (Keentok, 1982; Nguyen and Boger, 1983). As well, the assumption is made that the material yields *instantaneously* along the cylindrical surface at the maximum torsional moment (Nguyen and Boger, 1983). Under these assumed conditions, the stress on the cylindrical and flat end surfaces described by the rotating vane is equal to the yield stress (σ_y) at the maximum torsional moment (T_m) and Equation 2.9 is reduced to,

$$T_m = \pi \sigma_y \left[\frac{D^2 H}{2} + \frac{D^3}{6}\right]. \tag{2.10}$$

Nguyen and Boger (1983; 1985) concluded that the assumption of a uniform shear stress distribution over the end surfaces is valid for vanes of very small diameters (as D approachs 0). In practice, vanes have a finite diameter and there will then be some error made in calculating yield stress using Equation 2.10. The following equation, proposed by Nguyen and Boger (1983), can be used to approximate the error involved in making this assumption:

$$T_m = \frac{\pi D^3}{2}\left[\frac{H}{D} + \frac{1}{m+3}\right]\sigma_y \tag{2.11}$$

where m is a constant describing the radial distribution function of σ_e. When $m = 0$, Equation 2.11 becomes Equation 2.10.

A second method proposed by Nguyen and Boger (1985) recommends using vane fixtures of varying lengths but which have the same diameter, therefore, the second term in Equation 2.9 is constant. The yield stress can then be calculated from the slope of the plot of peak torque versus vane height.

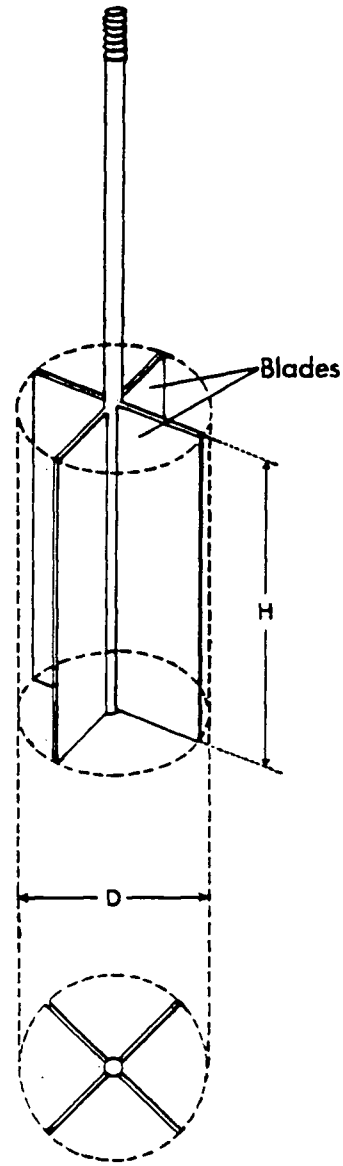

Figure 2.5: Diagram of a vane fixture used to measure yield stress. The vane shown has a blade height of 40.0 mm, and four blades of diameter 25.0 mm (to scale).

Chapter 3

EXPERIMENTAL

3.1 CHOCOLATE SAMPLES

3.1.1 Product Description

Two commercial chocolate samples, Hershey Milk Chocolate and Hershey Special Dark chocolate (Hershey Chocolate Company, Hershey, PA) and two 5 kg blocks of experimental chocolate products were obtained directly from the Hershey Chocolate Company for use in this study. Of the two commercial samples, one was a milk chocolate and the other was a semi-sweet type chocolate. The milk chocolate contained sugar, milk, cocoa butter, chocolate, soya lecithin and vanillin. The semi-sweet chocolate contained sugar, chocolate, cocoa butter, soya lecithin and natural flavor. The ingredient list for the block samples was not provided, and they were marked as simply Hershey-1 and Hershey-2 and are referred to as H1 and H2 in this investigation. The commercial milk and semi-sweet products have been coded HMC and HSS, respectively.

3.2 CHEMICAL ANALYSES

The four chocolate products were analyzed for moisture, ash, crude protein, fat and sucrose content. Prior to chemical analysis, composite chocolate samples were finely grated and stored in airtight containers until used. Samples were tested in triplicate for each analysis.

3.2.1 Moisture

Moisture was determined for each chocolate sample using a modified AOAC Method 13.002 for cacao products (AOAC, 1984). The samples (2 g) were weighed accurately into twelve predried, desiccator-cooled, weighed aluminum pans (60 mm diameter, 18 mm depth). The samples were placed in a vacuum oven at 100°C and 100 kPa for 12 hours. The samples were cooled in a desiccator containing silica gel, and then weighed. The samples were returned to the oven for an additional hour, cooled and reweighed. No change in weight was observed in the second drying period, thus the the loss in weight compared to the original sample weight was reported as percent moisture.

3.2.2 Ash

The ash content was determined using AOAC Method 13.005 for cacao products (AOAC, 1984). The ground chocolate samples (3 g) were accurately weighed into twelve 50 mL porcelain crucibles previously heated (lids included) to 600°C, cooled in a desiccator, and weighed. The samples were placed in the furnace and the temperature slowly brought to 600°C over a period of four hours. The samples were then ashed overnight, cooled in a desiccator for one hour and weighed. They were returned to the oven for an additional hour, cooled and reweighed. The change in weight in the second high temperature treatment was negligible, so the ash content of each sample was calculated from the final weight of ash in comparison with the initial sample weight.

3.2.3 Crude Protein

Protein analysis was carried out using a micro-Kjeldahl technique (Concon and Soltess, 1973). Prepared samples were accurately weighed (0.10 g) into twelve clean 30 mL Kjeldahl flasks. A catalyst, 2.3 g of a K_2SO_4-HgO mixture (190:4, w/w), was added,

followed by 2.3 mL concentrated H_2SO_4. The samples were placed on heating elements and digested with periodic additions of small amounts of H_2O_2 until all organic material had oxidized and the clear solution was refluxing halfway up the neck of the flask. The solutions were removed from the heat, cooled and diluted to 15 mL with distilled deionized water. An aliquot of each solution was analyzed for nitrogen content using a Technicon Autoanalyzer (Technicon Industrial Systems, Tarrytown, NY). Crude protein content was then calculated by multiplying nitrogen content by a factor of 6.25.

3.2.4 Fat

The fat content was determined using a modified International Office of Cocoa and Chocolate - AOAC Method 13.032 for cacao products (AOAC, 1984). Prepared samples were accurately weighed (1 g) into twelve 250 mL beakers. To each beaker, 20 mL of boiling water was added slowly, while stirring, to give an homogeneous suspension. An additional 25 mL of 8M HCl was added, the beakers covered with watch glasses and the solutions gently boiled for 15 minutes. The digest was filtered through Whatman No. 542 filter paper. The beakers and watch glasses used were rinsed with water and the washings added back to each sample. The digest was washed until the filtrate was Cl-free as determined by adding a few drops of 0.1M $AgNO_3$. The samples, rolled up inside the wet filter paper and placed inside Whatman cellulose extraction thimbles (22 x 80 mm), were then placed inside glass support thimbles and dried in covered beakers for 12 hours in a oven at 100°C.

The digestion beakers, drying beakers and watch glasses were rinsed with petroleum ether and the washings poured through each thimble and collected in 100 mL Labconco extraction flasks. The flasks had been previously dryed for 1 h at 100°C, cooled in a desiccator and weighed prior to use. The thimbles, containing dried sample, and the extraction flasks were placed into the Goldfisch extractor (Labconco Corporation, Kansas

City, MO). Additional petroleum ether was added to each flask to make up approximately 30 mL and the samples gently refluxed overnight to complete extraction. The flasks were removed from the extractor and placed in a fume hood until the solvent had been expelled. The flasks were then dried at 100°C for 2 hours, cooled in a desiccator and weighed. No change in weight was observed after an additional drying period of 1 hour and the fat content of each sample was calculated.

3.2.5 Sucrose

The sucrose content was determined using AOAC Method 13.054 for cacao products (AOAC, 1984). This procedure was modified to accommodate a smaller sample size. As well, only a direct polarization was carried out. Prepared samples (5 g) were accurately weighed into twelve 250 mL Nalgene centrifuge bottles each containing 50 mL of petroleum ether. The bottles were capped, the samples mixed for 5 minutes and centrifuged for 10 minutes at 4,080 x g. The extraction was repeated and the bottles placed in a fume hood until the petroleum ether had been expelled. The defatted samples were mixed with 50 mL of water and the bottles immersed in a water bath set at 90°C. The bottles were removed from the bath, cooled and approximately 1 mL of *basic* $Pb(OAc)_2$ solution (C.P. Bakers Analyzed), with a specific gravity of 1.25, was added to complete precipitation. The samples were mixed thoroughly, centrifuged and the supernate decanted through filter paper (Whatman No. 4). Any excess Pb was precipitated out using $K_2C_2O_4$ and the solutions filtered again. The pH of the twelve test solutions was measured and fell between pH 7.0 and 7.5. Each sample was then polarized in a 100 mm tube at 20°C at a wavelength of 589 nm using a Perkin-Elmer 141 polarimeter (Perkin-Elmer Corporation, Norwalk, CT). The sucrose content of the samples can be calculated from the measured degree of optical activity in the prepared solutions.

3.3 PARTICLE SIZE ANALYSIS

The mean particle size and particle size distribution of the four chocolate samples were determined using a Coulter Counter Model TAII (Coulter Electronics Inc., Hialeah, FL) An experimental procedure was developed following recommendations outlined by Robbins (1983). Robbins did not recommend defatting the samples prior to analysis. An electrolyte solution of 5% ammonium thiocyanate (Fisher Certified A.C.S.) and absolute ethanol was prepared and clarified by centrifugation in 250 mL stainless steel cups at 4,080 x g for 30 minutes. Sample suspensions were made by mixing 0.15 g of sample in 20 mL electrolyte solution in new (dust free) Simport 20 mL dilution vials. One drop of Tween 20 was added to each vial to aid in breaking up aggregates of particles. The suspensions were sonicated for two minutes (Bransonic 220, Branson Instruments Co., Shelton, CO) prior to analysis in order to ensure complete dispersal of the sample in electrolyte. Samples were tested in duplicate and three runs were taken for each sample.

3.4 YIELD STRESS DETERMINATION

The flow properties of chocolate melts can be determined by either indirect or direct methods, as previously described. Using the indirect method, yield stress was estimated by fitting the Casson equation to shear stress-shear rate data and extrapolating to zero shear rate. Direct methods of measurement used were the Stress Relaxation Method, the Single Vane Method and Multiple Vane Method I and Method II.

3.4.1 Calibration

The calibration of each of the three rheometers used in this study was checked prior to use. The form factors, which relate torque to shear stress and rotational speed to shear rate, listed in the operation manuals, were verified using standard oils and recalculated

if necessary.

The Brookfield HAT viscometer (Brookfield Engineering Laboratories, Stoughton, MA) was checked using two Brookfield viscosity standards consisting of silicone oil fluids of known viscosity at 25°C. The viscosity values obtained experimentally were in close agreement with that of the standard used.

The Brabender Rheotron viscometer (C.W. Brabender Instruments Inc., South Hackensack, NJ) with coaxial cylinder fixtures A1 and A2 was calibrated using a certified viscosity standard, S600, (Cannon Instrument Company, State College, PA) at 20°C using coaxial cylinder fixture A1. This instrument no longer conformed to the parameters given in the manual and the shear stress factors for springs A, B and C were recalculated. The method used included a correction factor for end effect. As well, the operating speeds on the Brabender were checked and found to differ from those printed on the control unit. These new speeds (rpm) were used in the calculation of new shear rate values for fixtures A1 and A2.

The Carri-Med Controlled Stress rheometer (Carri-Med Limited, Dorking, UK) with coaxial cylinder fixture 5222 was calibrated using the Cannon standard oil, S600, at 20°C. The calibration, which included a correction for end effect, was calculated and applied to the stress factor. The instrument parameters are listed in Table 3.1.

3.4.2 Sample Preparation

The chocolate samples were prepared for rheological testing as recommended by the International Office of Cocoa and Chocolate (OICC, 1973). Composite samples were cut into 5 gram pieces or smaller. Approximately 125 grams of each grated sample was placed in 300 mL beakers covered with foil and heated in an incubator oven set at 55°C. The chocolate was stirred by hand with a rubber tipped stirring rod at intervals using a stirring rate not exceeding 60 revolutions per minute until the chocolate had completely melted

Table 3.1: Instrument parameters for the coaxial cylinder fixtures used.

Instrument	Cylindrical Fixtures	Form Factors		Bob/Cup Radius Ratio (a)
		Shear Stress (Pa)	Shear Rate	
Brookfield	SC4-27/13R	17.0	0.34	0.62
Brabender	A1, spring A	0.0198	2.985	0.964
	B	0.1209		
	C	1.3016		
	A2, spring A	0.0231	1.033	0.893
	B	0.1410		
	C	1.5182		
Carri-Med	5222	0.010	9.751	0.892

and reached a temperature of 50°C as determined by a calibrated thermocouple. The thermocouple used was a Teflon-coated, Type J iron/constantan wire pair with a soldered junction and readout provided by a digital temperature indicator meter (C.W. Brabender Instruments, Inc., South Hackensack, NJ). The thermocouple and digital readout system was calibrated against an ASTM certified thermometer.

The time taken in the oven for the sample to completely melt and reach a temperature of 50°C was determined to be between 15 and 25 minutes. All fixtures were preheated in the incubator for five minutes prior to testing. The spindle or vane fixture was then attached to the torsion head of the rheometer, and the sample gently poured into the cup and loaded into the instrument. Temperature in the sample was maintained at 40°C with a thermostatically controlled water supply circulating in a water jacket around the sample cup. The chocolate was brought to 40°C while shearing the sample at a rate between 5

and 25 s^{-1}. The sample temperature was monitored using the thermocouple. The time required to reach 40°C was determined to be 15 minutes for the larger sample volume required by the Brabender Rheotron and 10 minutes for the smaller sample volume used with the Brookfield and Carri-Med rheometers.

3.4.3 Indirect Methods

The Casson Model equation was fitted to the experimental shear stress-shear rate data obtained from each of the three rheometers used in this investigation. Shear stress (σ, Pa) and shear rate ($\dot{\gamma}$, s^{-1}) values were calculated from the mean scale readings using the calibration data, form factors and rotational speeds. The appropriate non-Newtonian shear rate correction factor specific to the coaxial cylinder fixture used was applied to each data set. Least squares linear regression was used to obtain the equation for the Casson model and related parameters for each set of flow data.

Brookfield Viscometer

Flow measurements of each chocolate sample were made using the Brookfield HAT viscometer with the small sample adapter consisting of the SC4-13R water jacketted sample chamber or cup with the SC4-27 cylindrical bob. Scale readings were taken at 1.0, 2.5, 5, 10, 20 and 50 rpm using first the ascending, then descending order of speeds. These speeds represented a shear rate range of approximately 0.34 to 17.0 s^{-1}. With the one viscometer and fixture combination it was not possible to obtain readings for all speeds. For example, readings were off scale at 50 rpm for HMC and HSS and at both 20 and 50 rpm for H1. A total of twelve samples was tested in a random order.

Brabender Rheotron Viscometer

Two coaxial cylinder fixtures, A1 and A2, of differing gap width were used with the Brabender Rheotron to evaluate the rheological behavior of the chocolate melts. Scale reading measurements were taken at eleven discrete speeds using the A1 fixture and twelve discrete speeds using the A2 fixture, representing shear rate ranges of approximately 0.19 to 75.8 s^{-1} and 0.07 to 50.8 s^{-1}, respectively. Using a stripchart recorder, the torsion signal was monitored at each speed and readings were recorded when an equilibrium value was reached. Again, readings were taken in an ascending then descending order over the range of speeds used for each fixture. The twelve samples were tested in a random order using the A2 coaxial cylinder fixture first, followed by the A1 coaxial cylinder fixture.

Carri-Med Controlled Stress Rheometer

The Carri-Med Controlled Stress Rheometer was used with coaxial cylinder fixture 5222 to evaluate the flow properties of the four chocolate samples. Operation of the rheometer was controlled through a microcomputer interfaced to the instrument. In preparation for testing, the sample was loaded manually, and sheared at a low constant stress for 10 minutes while the temperature of the sample equilibrated prior to testing.

The sample cup which was supported on a pneumatic ram, automatically rose to bring the sample up to surround the spindle which was attached to the drive motor, when the switch was turned on or when instructed through the computer. This ram action was found to be too abrupt, thereby forcing some of the sample to spill out of the cup and possibly introducing air bubbles into the sample. A satisfactory solution was found when the distance between the sample cup and the spindle was increased by adjusting the micrometer wheel on the lower ram assembly. Then, when the ram switch

was activated, the sample cup rose and the spindle was immersed only part way into the sample. Turning the micrometer wheel, the cup was slowly moved up until the spindle was fully immersed in the sample. The bottom gap width was set to 1.5 mm before each test run.

The spindle was rotated through a programmed loop of increasing and then decreasing stress for 10 minutes. This represented shear rate ranges of approximately 0 to 10 s^{-1}, 0 to 40 s^{-1}, 0 to 20 s^{-1} and 0 to 50 s^{-1} for HMC, HSS, H1 and H2, respectively. Duplicate samples were evaluated in random order with two consecutive runs taken for each sample. A second test was conducted in which the effect of run time was studied in relation to the yield stress measured. Two procedures consisting of run times of 12 and 30 minutes were used on triplicate samples of H2 and H1.

3.4.4 Direct Methods

Stress Relaxation Method

The Brabender Rheotron with coaxial cylinder fixtures A1 and A2 were used for direct measurement of yield stress using the stress relaxation method. The sample was brought to an equilibrium condition by shearing for a 30 minute period at 0.064 rpm. Not all samples required a 30 minute period to reach an equilibrium state, but this length of time was chosen because it represented the maximum amount of time required and all samples would be tested in the same manner.

Two procedures for stress relaxation were used. In the first procedure, a single measurement was taken after shearing the samples for 10 minutes, turning off the drive motor, and recording the residual stress remaining in the sample using a stripchart recorder. When measurements recorded over a 10 to 15 minute period were virtually unchanged, these values were taken to represent the yield stress of the sample.

The test samples in the second procedure were sheared at speeds of 0.064, 0.120 and 0.224 rpm for 10 minute intervals. The drive motor was then turned off and the residual stress remaining, after shearing at each rotational speed, was recorded using a stripchart recorder. Again, measurements recorded over a 10 to 15 minute period were virtually unchanged and these values were taken to represent the yield stress of the sample. Replicate samples were tested in a random order using the A2 fixture first and then the A1 fixture. The speeds were randomized within each sample and fixture combination.

Vane Fixture Method

Direct yield stress measurements can also be made using the vane fixture method (Nguyen and Boger, 1983). A series of 4-bladed vane fixtures was constructed for these experiments as shown in Figure 2.5 with dimensions as given in Table 3.2. Based on recommendations of Nguyen and Boger (1985) vane fixtures E, F and G were chosen for testing. In addition, two larger vanes, K and O, were used, although they did not meet all of the dimensional criteria described in the procedure outlined by Nguyen and Boger.

A selected vane fixture was attached to the torque sensing unit of the Brabender Rheotron and the sample carefully loaded into the A-series cup (56 mm diameter). Once the sample had reached the equilibrium test temperature of 40°C, a constant speed was applied while the torsion signal during the start-up of rotation was recorded on a potentiometric stripchart. The maximum or peak torque recorded was converted to a stress value using the torsion spring constant and surface area within the sample sheared at the surface of a cylindrical volume described by the length and diameter of the vane fixture. This peak stress was taken as an estimate of the yield stress. Relaxation stresses in the sample were also recorded; however, residual readings were negligible using this type of fixture with the Brabender viscometer.

Table 3.2: Vane fixture dimensions

Vane Fixture	Vane Height (cm)	Vane Diameter (cm)	Ratio H/D
E	4.0	1.5	2.6
F	4.0	2.0	2.0
G	4.0	2.5	1.6
K	5.5	2.5	2.2
O	7.0	2.5	2.8

Preliminary tests showed a dependence of the peak torque value measured on the rotational speed used. Torque values appeared to be relatively constant at very low speeds, but they increased significantly at tested speeds of between 0.849 and 8.36 rpm, probably due to inertial effects on sudden start-up. As well, another preliminary test was conducted in which the peak torque was measured immediately upon loading the sample and after shearing the sample for 15 minutes at 0.064 rpm. No significant difference was observed ($p>0.05$) in a comparison of results from test samples. However, a 15 minute shearing period was included so that sample treatment was uniform and more closely related to pretest handling of samples used in the other methods.

Spring A was used in the torque sensor of the instrument to provide greater sensitivity to the stress generated using the vane fixtures. Rotational speeds of 0.064, 0.120 and 0.224 were selected for the test procedure. The peak torque values were measured for duplicate samples using the five vane fixtures, randomized within each sample, and rotational

speeds were randomized within each of the vane fixtures. The peak torque data were analyzed using the Single Vane Method and Multiple Vane Methods I and II as previously described.

3.5 DATA ANALYSES

The yield stress and viscosity estimates obtained using Brabender Rheotron were analyzed in a two-way analysis of variance (ANOVA) using a repeated-measures design to test for a significant difference between fixture types. This design was also used for the Carri-Med data obtained over consecutive runs as well as for the second data set where two different run times were used.

Data sets analyzed using Vane Methods I and II were tested for equality of lines using a multiple regression analysis. Since there was no significant difference between regression lines, the data were pooled and a two-way analysis of variance (ANOVA) was used to test for a significant difference in rotational speeds used. Yield stress estimates obtained using the conventional vane method were analyzed using a split-plot design. All statistical procedures used (Steel and Torrie, 1960) were calculated using the BMDP program (Dixon, 1985) on the UBC Amdahl 5860 computer. Graphical presentation of the data was performed using the Tell-A-Graf graphics program also available on the UBC mainframe computer.

Chapter 4

RESULTS AND DISCUSSION

4.1 CHEMICAL ANALYSES

A proximate analysis, consisting of moisture, ash, fat and protein determinations, was carried out on each chocolate sample. An estimate of total carbohydrate was derived from the difference. Also, since it is known that chocolate has a high sugar content, the sucrose content of each sample was determined. All analyses were carried out to characterize the test material and provide some insight into the differences in flow properties observed between test samples.

The compositions of the four chocolate samples are given in Table 4.3. The relative amounts of moisture, fat, protein and sucrose found in the test materials were similar to values reported in the literature for other dark and milk chocolate formulations. The moisture content was low for all samples tested, ranging from 0.92% for H2 to 1.84% for HMC. Previous studies have shown how the water content can influence viscosity and yield stress. Researchers found that viscosity did not vary significantly over a range of 0.6 - 1.1% moisture, whereas yield stress increased steadily as moisture content increased (Chevalley, 1975).

The ash content of the samples varied between 1.22% for HSS to 1.65% for H1 and HMC; H2 was slightly less at 1.54%. The higher ash values may be due to milk in the Hershey milk chocolate as well as in the other two. Although it is not known what ingredients were used in the manufacture of H1 and H2, the light color and flavor of the

Table 4.3: Composition of the chocolate samples.

Analysis	Composition of Sample (%)			
	HMC	HSS	H1	H2
Moisture	1.84	1.22	1.67	0.917
Ash	1.65	1.22	1.65	1.54
Fat	31.8	30.8	30.1	32.1
Protein	6.75	4.91	6.99	6.44
Carbohydrate‡	58.1	61.9	59.5	59.1
Sucrose	49.7	52.1	50.1	50.0

‡- [100 - (total of other components)]

chocolate suggested the presence of milk. HSS was a semi-sweet chocolate and did not contain milk.

Samples H2 and HMC contained the most fat at 32.1% and 31.8%, respectively. HSS contained 30.8%, which was approximately 1.0% less, and, H1 contained 30.1% fat, a difference of 2.0% as compared to H2. Generally, the fat content of chocolate is in the range of 28 - 40% (Tscheuschner and Markov, 1986). An inexpensive chocolate may contain between 22 - 28% fat (Niediek, 1980).

The protein content of chocolate is not high. Milk chocolate has a slightly higher protein content than dark chocolate due to the presence of milk protein. Of the four samples analyzed, H1 had the highest protein content of 6.99%. HMC and H2 had slightly lower amounts at 6.75 and 6.44%, respectively. The semi-sweet chocolate, HSS contained approximately 2.0% less protein than the other samples at 4.91%.

Total carbohydrate was estimated by the difference between 100 and the percent totals of the other components. Chocolate is a rich source of carbohydrate of which a large proportion is comprised of sucrose. The samples were found to contain, in increasing order, 49.7, 50.0, 50.1 and 52.0% sucrose for HMC, H2, H1 and HSS, respectively.

A multivariate analysis of variance (MANOVA), using the BMDP:4V statistical software program, was used to test for significant differences among samples. The samples differed significantly in chemical composition (Table 4.4), and the univariate statistics showed that each chemical analysis was significantly different between chocolate samples tested.

4.2 PARTICLE SIZE ANALYSIS

A Coulter Counter Model TAII was used to analyze the particle size distribution in each of the four chocolate samples. The pooled mean particle size determined for each

Table 4.4: Multivariate analysis of variance for chemical composition.

Variate	df	Mean Square	F-Ratio
Sample	15	0.5288E-05^{w}	46.63 **
Ash	3	0.1255	19.83 **
Error	7	0.0063	
Moisture	3	0.4447	402.6 **
Error	7	0.0011	
Fat	3	2.0856	7.010 *
Error	7	0.2975	
Protein	3	2.6088	49.06 **
Error	7	0.0532	
Sucrose	3	3.7082	20.48 **
Error	7	0.1810	

w - Wilks' lambda likelihood ratio statistic.
* - significant at $p<0.05$ ** - significant at $p<0.01$

Table 4.5: Range and mean sizes of particles in the chocolate samples.

Sample	Pooled Mean (μm)	Coefficient of Variation (%)	Size Range (μm)
HMC	6.98	6.93	2.5 - 80.5
HSS	5.73	2.22	2.5 - 80.5
H1	6.27	4.21	2.5 - 64.0
H2	7.15	11.01	2.5 - 80.5

chocolate is given in Table 4.5. Sample HSS had the smallest average particle size of 5.73 μm, followed by H1 with a mean size of 6.27 μm and HMC and H2 with mean particle sizes of 6.98 and 7.15 μm, respectively. Figure 4.6 shows the percentage of particles at sizes ranging from 2.5 to 25.5 μm. Larger sized particles between the sizes of 25.5 and 80.5 μm accounted for less than 1% of the total population.

Generally, for chocolate, the particle size of the sugar crystals ranges from 5 to 35 μm and the particle size of the cocoa solids from 15 to 20 μm (Tscheuschner and Markov, 1986). In this analysis, the greatest number of particles appeared to be in the range of 4.0 to 5.0 μm. Approximately 70 and 80% of the total population of particles, for samples H1 and HSS, respectively, lie within this size range. For samples HMC and H2 the numbers are lower at 60 and 65%, respectively and these samples have a broader particle size distribution. Overall, these results were similar to Coulter analysis data reported in the literature (Malm, 1967; Minifie, 1980).

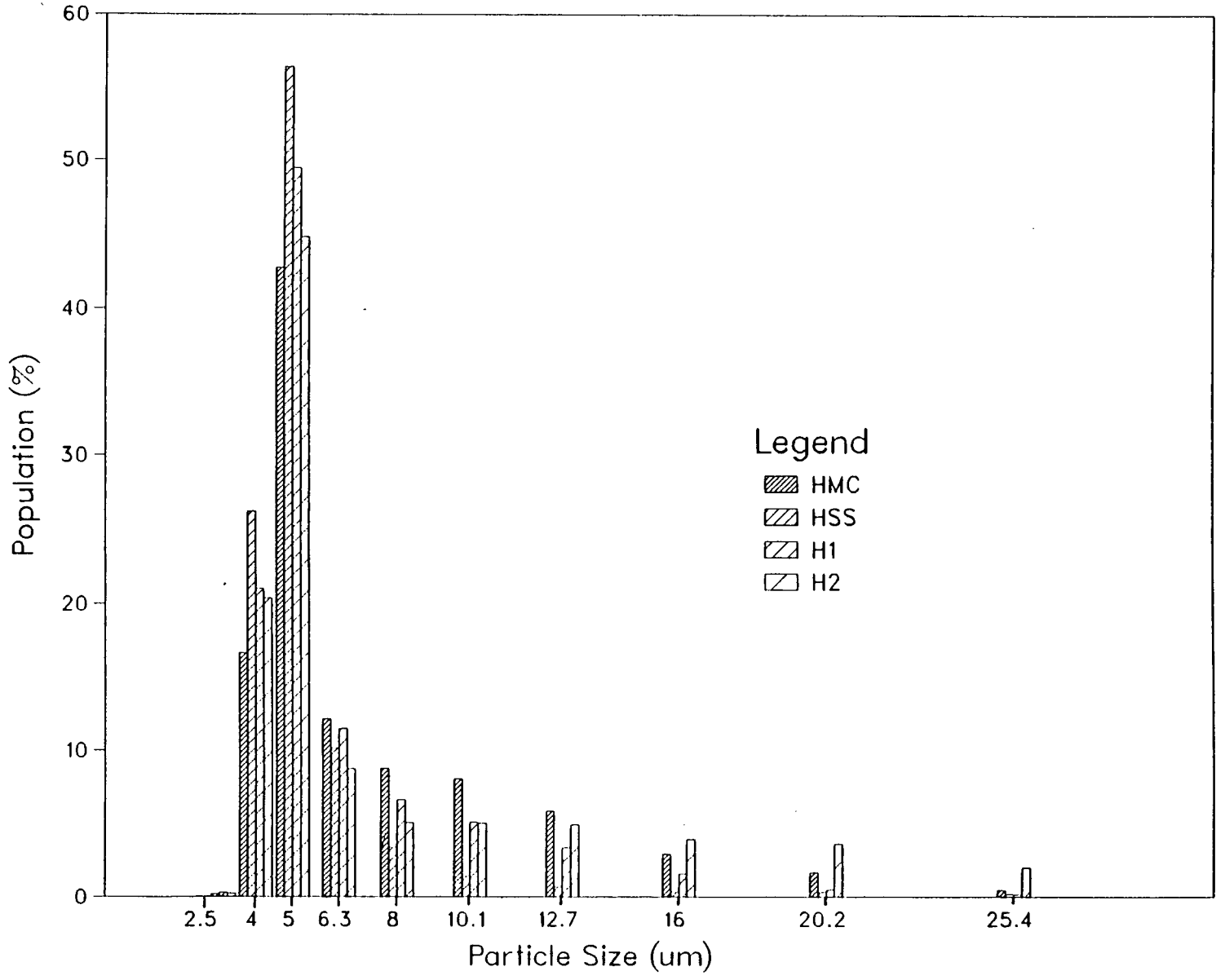

Figure 4.6: Distribution of sizes for particles contained in the chocolate samples

4.3 INDIRECT ESTIMATION OF YIELD STRESS

4.3.1 Brookfield Viscometer

The Brookfield HAT viscometer was one of three rotational viscometers used in this investigation to determine the flow properties of the four chocolate samples. The samples were prepared and tested following the OICC methodology as described previously. The Casson equation was fitted to the shear stress-shear rate data and the appropriate non-Newtonian shear rate correction factor applied.

The rheograms for each chocolate type are shown together in Figure 4.7 as the square root of shear stress vs the square root of shear rate. A good straight line fit would indicate that flow followed the Casson model, and in each case this was true with the exception of sample H1. The rheogram for sample H1 showed a marked curvature towards the abscissa. The Casson flow parameters for each chocolate sample are listed in Table 4.6. Yield stress values ranged, in order of increasing magnitude from 9.38 Pa for HMC, 9.59 Pa for H1, 10.6 Pa for H2, to 19.8 Pa for HSS. Correspondingly, Casson viscosity estimates were 10,010, 19,300, 4,500 and 5,270 mPa·s for HMC, H1, H2 and HSS, respectively The coefficients of variation for all samples tested were below 10%.

Although the SC4-27/13R fixture is recommended for use with the Brookfield HAT viscometer for testing molten chocolate, the maximum shear rate obtainable was 17.0 s^{-1}. This does not meet the maximum shear rate of 60 s^{-1} recommended by the OICC. Also, the recommended bob to cup ratio (a) is 0.65 or greater. This ratio is 0.62 for the Brookfield fixture. However, the Casson rheograms for 3 of the 4 samples tested were linear, indicating that this model applied to the data over the shear rate range tested using a coaxial cylinder fixture with a wider gap width. Sample H1 was very viscous and a higher yield stress estimate was expected. At the lower shear rates, it is possible that this sample was not being sheared across the entire gap. As well, the sample could be

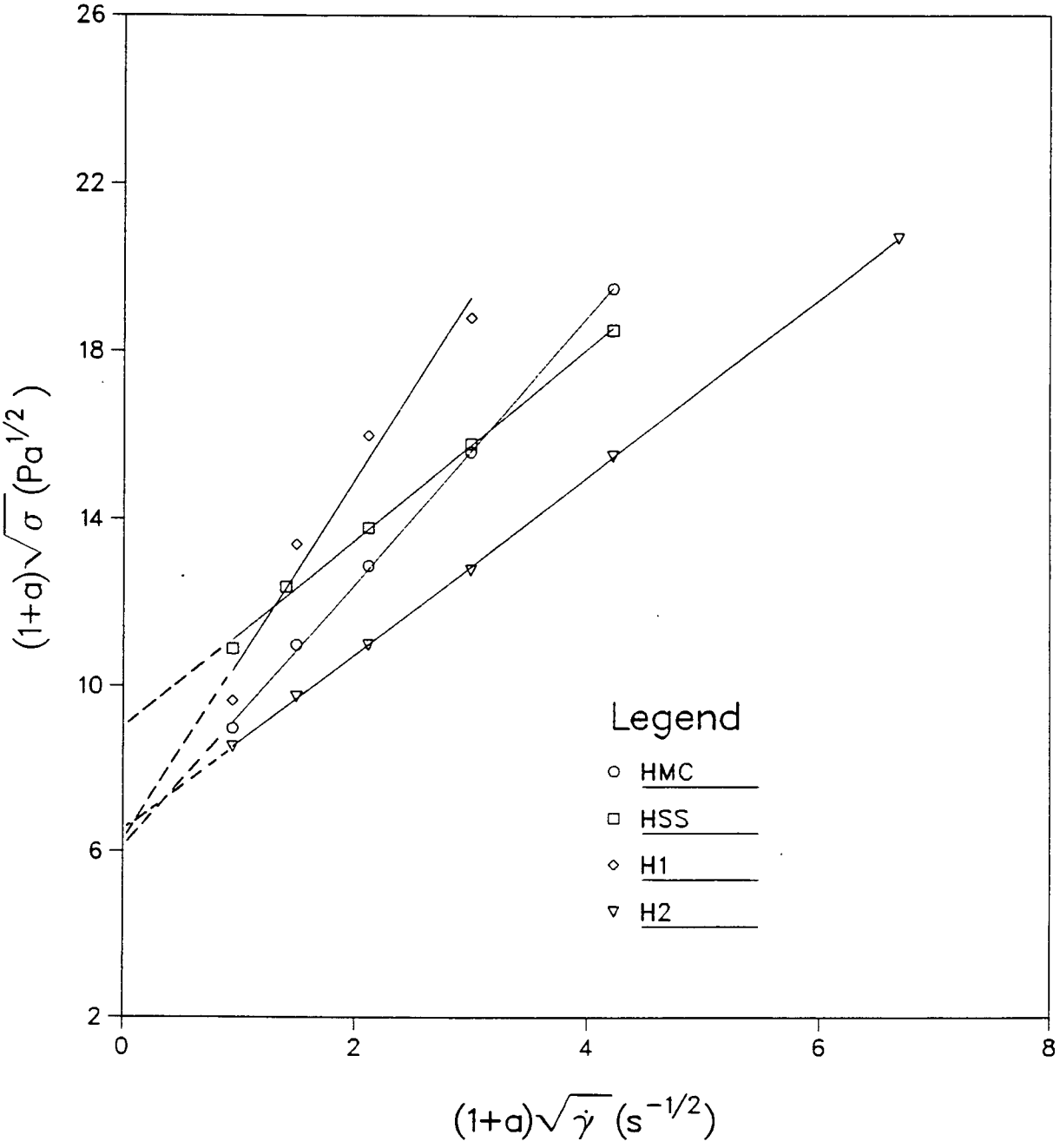

Figure 4.7: Casson flow curves of chocolate samples at 40°C obtained with the Brookfield HAT Viscometer using the SC4-27/13R bob and cup fixture.

Table 4.6: Casson flow parameters for chocolate melts at 40°C obtained with the Brookfield HAT viscometer using the SC4-27/13R bob and cup fixture.

Sample	Casson Parameters		Coefficient of Determination, r^2
	σ_{ca}, (Pa)	η_{ca}, (mPa·s)	
HMC	9.38 (8.45)†	10110 (3.68)	1.000 (n=5)
HSS	19.8 (4.53)	5270 (2.82)	0.999 (n=5)
H1	9.59 (6.57)	19300 (2.61)	0.970 (n=4)
H2	10.6 (1.47)	4510 (1.58)	1.000 (n=6)

†- Coefficient of variation (%)

slipping at the fluid/fixture contact surfaces. Both would contribute to a lower apparent yield stress estimate.

The National Confectioners Association (Sequine, 1986) recommended a minimum a ratio of 0.60 along with a minimum speed of 5 rpm (1.7 s^{-1}) at which to shear the sample, in that the conditions outlined by Steiner, for the correct use of the Casson equation, would be satisfied. If these guidelines were followed, only two data points could then be used to plot a rheogram for sample H1, at 5 and 10 rpm; readings were offscale at 20 and 50 rpm (see Appendix A). Data below 5 rpm, at 2.5 and 1.0 rpm, for the other samples showed no deviation from linearity and were included in the calculations for the Casson flow parameters.

4.3.2 Brabender Rheotron Viscometer

The steady shear Casson flow behavior of the chocolate samples was determined using the Brabender Rheotron viscometer and coaxial cylinder fixtures A1 and A2. The flow parameters are listed in Table 4.7. These values were similar to those obtained using the Brookfield instrument, with the exception of sample H1. The yield values, in particular, were slightly higher for the Brabender viscometer tests, and were greater for the A1 fixture as compared to those obtained using the A2 fixture, again with the exception of sample H1. Conversely, the viscosity values were lower for the A1 fixture as compared to the A2 fixture for all samples. Coaxial cylinder fixture A1 had a smaller gap width than fixture A2. The variation coefficients were below 10% for all samples tested except for the viscosity value measured for sample H1 using the A2 fixture.

Analysis of variance results in Tables 4.8 and 4.9 using the BMDP:2V program (for repeated measures) indicated that fixture and fixture x sample interaction significantly ($p<0.01$) influenced yield stress and viscosity values. The discrepancy in yield values between the two fixtures may be due to a combination of plug flow and/or wall slip.

Slip effects were reported to occur in chocolate tested with coaxial cylinder fixtures (Steiner, 1962). Chocolate yield values measured using wide and narrow gap fixtures with a Haake Rotovisco viscometer were higher for the narrow gap fixture. Although Charm (1963) reported from unpublished data that there was no difference between fixtures of varying gap widths when measuring yield stress of chocolate, he did find differences for applesauce and tomato puree. In other fluid-like materials, problems due to slip when using coaxial cylinder fixtures have been widely reported in the literature (Cloud and Clark, 1985; Yoshimura and Prud'homme, 1988; Kiljanski, 1989; Qui and Rao, 1989). The gap width of the coaxial cylinder fixture, as well as the test material, may influence the magnitude of these effects.

Table 4.7: Casson flow parameters for chocolate melts at 40°C obtained with the Brabender Rheotron using coaxial cylinder fixtures A1 and A2.

Sample	Fixture	Casson Parameters		Coefficient of Determination, r^2
		σ_{ca}, (Pa)	η_{ca}, (mPa·s)	
HMC	A1	15.7 (8.10)†	7325 (1.71)	0.997 (n=11)
	A2	12.3 (3.45)	8770 (0.58)	0.998 (n=12)
HSS	A1	29.3 (0.82)	4486 (3.68)	0.995 (n=11)
	A2	24.0 (2.24)	4952 (1.64)	0.993 (n=12)
H1	A1	29.7 (3.18)	6171 (0.60)	0.996 (n=11)
	A2	30.4 (7.11)	8748 (12.2)	0.989 (n=12)
H2	A1	17.5 (8.18)	3942 (6.78)	0.994 (n=11)
	A2	17.2 (4.44)	4411 (5.52)	0.994 (n=12)

† - Coefficient of variation (%)

Table 4.8: Analysis of variance for Casson yield stress obtained with the Brabender Rheotron using coaxial cylinder fixtures A1 and A2.

Source of Variation	df	Mean Square	F-Ratio
Sample	3	344.43	122.0 *
Error	8	2.8238	
Fixture	1	25.359	23.84 *
Interaction			
Fixture x Sample	3	11.227	10.55 *
Error	8	1.0637	

* - significant at $p<0.05$

Table 4.9: Analysis of variance for viscosity obtained with the Brabender Rheotron using coaxial cylinder fixtures A1 and A2.

Source of Variation	df	Mean Square	F-Ratio
Sample	3	224.99E05	84.86 **
Error	8	265.13E03	
Fixture	1	921.78E04	39.77 **
Interaction			
Fixture x Sample	3	151.09E04	10.55 *
Error	8	231.77E03	

* - significant at $p<0.05$ ** - significant at $p<0.01$

Table 4.10: Casson yield stress estimates for chocolate samples at 40°C recalculated over the linear portion of the rheograms obtained with the Brabender Rheotron using coaxial cylinder fixtures A1 and A2.

Sample	Fixture	Yield Stress σ_{ca}, (Pa)	Coefficient of Determination, r^2
HMC	A1	16.0 (7.44)†	0.997 (n=10)
	A2	12.9 (2.33)	0.998 (n=10)
HSS	A1	30.1 (0.67)	0.994 (n=10)
	A2	25.6 (2.75)	0.995 (n=10)
H1	A1	33.2 (1.90)	0.997 (n=9)
	A2	38.1 (2.48)	0.997 (n=9)
H2	A1	18.0 (6.06)	0.994 (n=10)
	A2	17.2 (3.87)	0.993 (n=10)

† - Coefficient of variation (%)

The rheograms for steady shearing flow of chocolate melts produced using fixtures A1 and A2 are shown in Figures 4.8 and 4.9. There was a marked curvature towards the x-axis at the lower shear rates. Apart from slip, the shape of the rheograms suggested that the sample was deforming, but had not yielded to the shearing force applied. This deviation from linearity occurred below approximate shear rates of 0.3 to 0.5 s^{-1} for samples tested using the A2 fixture and 0.4 to 0.7 s^{-1} for samples using the A1 fixture. When these data points were removed and the Casson model fitted to the linear portion of the rheogram, higher yield stress estimates result (Table 4.10).

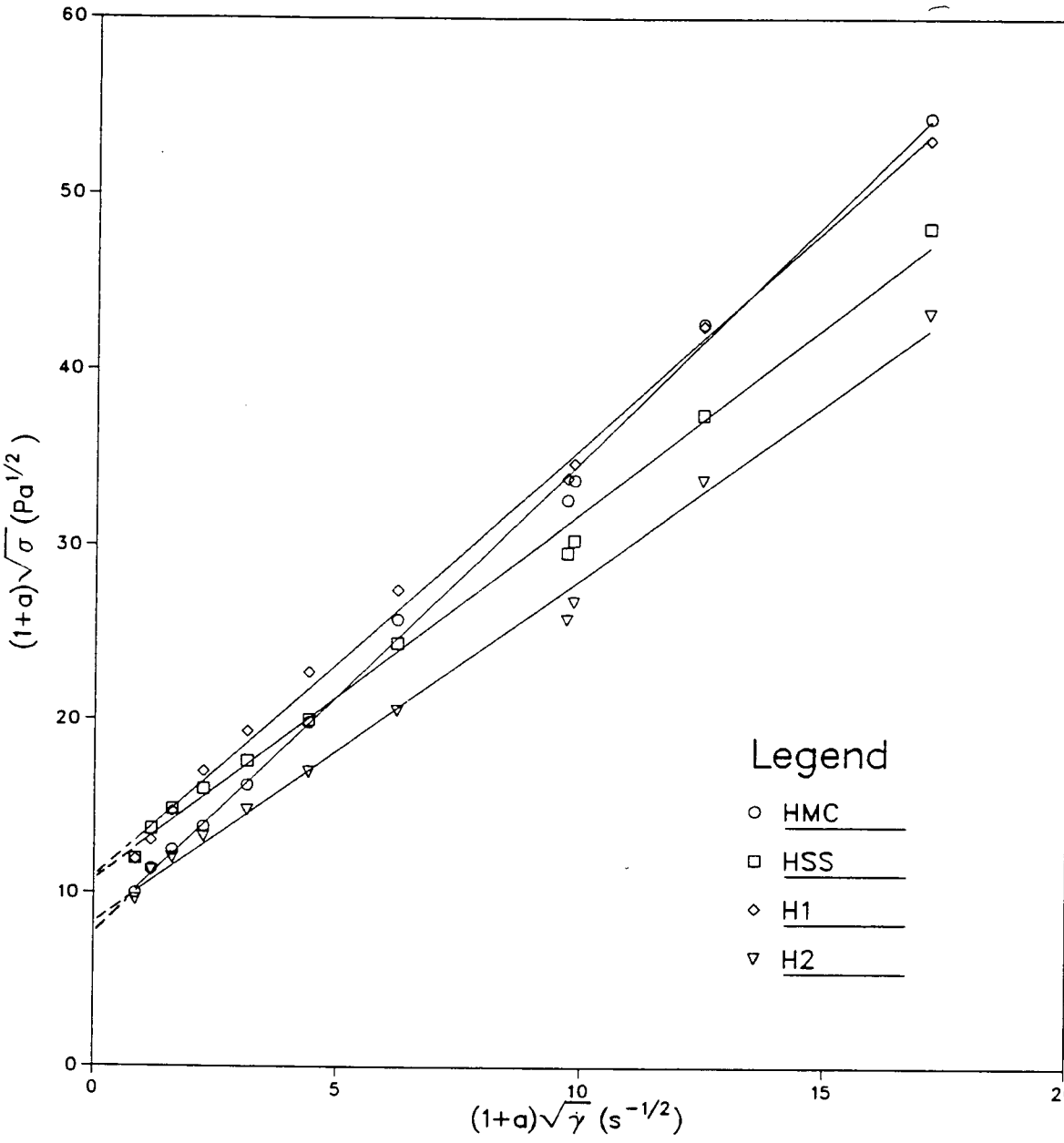

Figure 4.8: Casson flow curves of chocolate samples at 40° C obtained with the Brabender Rheotron viscometer using coaxial cylinder fixture A1.

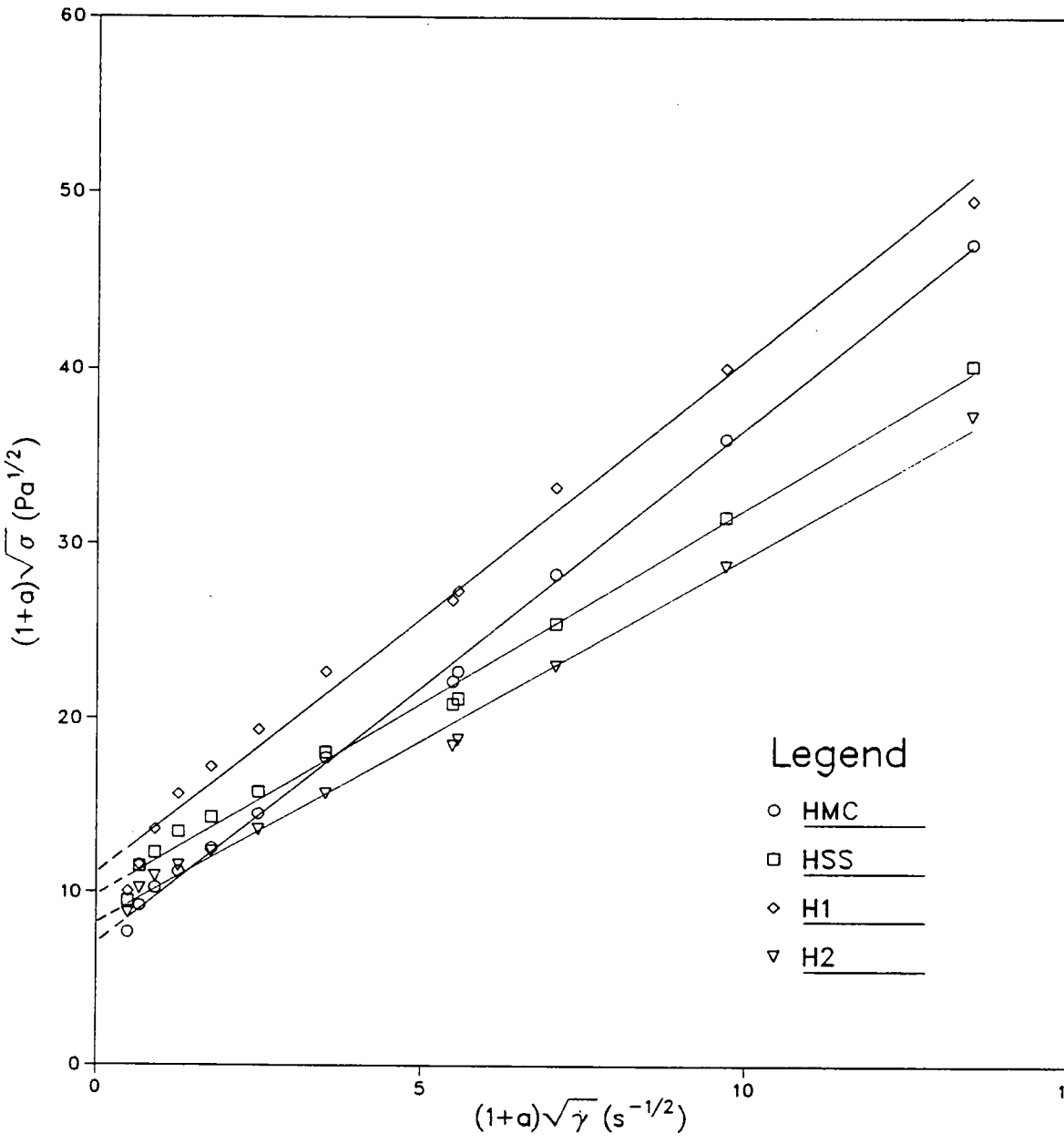

Figure 4.9: Casson flow curves of chocolate samples at 40° C obtained with the Brabender Rheotron viscometer using coaxial cylinder fixture A2.

4.3.3 Carri-Med Controlled Stress Rheometer

The Casson flow behavior of the chocolate melts was determined under controlled stress conditions using the Carri-Med rheometer. The mean Casson yield stress and viscosity estimates over two consecutive runs are listed in Table 4.11. The yield stress values did not vary significantly over consecutive runs (Table 4.12) but a significant difference was found for viscosity measurements (Table 4.13).

The yield values were comparable to those estimated from steady shearing flow using the Brabender viscometer. The largest discrepancy in yield value was for sample H1. A mean yield value of 23.5 Pa for H1 was measured using the Carri-Med as compared to 30.4 Pa obtained using the Brabender with the A2 fixture. The gap width of coaxial cylinder fixture 5222 used with the Carri-Med was the same as the A2 coaxial cylinder fixture.

The Casson viscosity estimates were higher for all samples when measured using the Carri-Med rheometer. This could be due to the testing procedure used. For a programmed run of 10 minutes, sample flow occurred over a narrower shear rate range in the Carri-Med rheometer as compared to the Brabender viscometer. The sample may not have *thinned out* as much as it could have had it been subjected to greater shear forces. The viscosity estimates obtained using the A1 and A2 fixtures with the Brabender also resulted in higher values measured for the A2 fixture where the maximum shear rate obtainable was less than the A1 fixture.

The Casson equation fitted the steady shear flow data, obtained with the Brabender, more accurately than the controlled stress data obtained with the Carri-Med. This may be due to the greater capability of the Carri-Med to measure flow continuously, when interfaced to a computer, and the ability to measure flow (or deformation) at lower rates of shear. Judging by the curvature of the rheograms (Figure 4.10), the molten chocolate

Table 4.11: Casson flow parameters for chocolate samples at 40°C obtained with the Carri-Med rheometer using coaxial cylinder fixture 5222.

Sample	Run	Casson Parameters		Coefficient of Determination, r^2
		σ_{ca}, (Pa)	η_{ca}, (mPa·s^{-1})	
HMC	1	13.4 (12.1)†	11020 (7.74)	0.964 (n=392)
	2	11.3 (0.04)	10500 (8.12)	0.995 (n=392)
HSS	1	21.0 (1.90)	5600 (0.49)	0.976 (n=388)
	2	20.1 (2.06)	5210 (4.04)	0.948 (n=387)
H1	1	23.3 (1.43)	11260 (1.16)	0.978 (n=388)
	2	23.6 (-)	11390 (-)	0.978 (n=385)
H2	1	19.9 (5.36)	10160 (16.8)	0.977 (n=388)
	2	18.4 (7.00)	10850 (17.4)	0.982 (n=389)

†- Coefficient of variation (%)

Table 4.12: Analysis of variance for Casson yield stress of chocolate samples at 40°C over consecutive runs obtained with the Carri-Med rheometer using coaxial cylinder fixture 5222.

Source of Variation	df	Mean Square	F-Ratio
Sample	3	75.410	84.68 **
Error	3	0.8905	
Run	1	4.5881	1.57 ns
Interaction			
Run x Sample	3	0.45082	0.15 ns
Error	3	2.9278	

* - significant at $p<0.01$ ns - not significant ($p>0.05$)

Table 4.13: Analysis of variance for Casson viscosity of chocolate samples at 40°C over consecutive runs obtained with Carri-Med rheometer using coaxial cylinder fixture 5222.

Source of Variation	df	Mean Square	F-Ratio
Sample	3	267.45E05	5.38
Error	3	496.82E04	
Run	1	114.59E04	25.53 *
Interaction			
Run x Sample	3	504.57E02	1.12 ns
Error	3	448.85E02	

* - significant at $p<0.05$ ns - not significant ($p>0.05$)

was deforming and/or slipping rather than flowing at apparent shear rates below 0.5 s^{-1}. Also, at these low shear rates, it was likely that plug flow was occurring. No flow could be detected below approximately 3.9 Pa for H1, 6.0 Pa for HMC and HSS and 8.5 Pa for H2. The lowest shear rate values measured were 0.05, 0.04, 0.03 and 0.06 s^{-1} for samples HMC, HSS, H1 and H2, respectively. Casson yield stress estimates recalculated over the linear portion of the rheograms were higher (Table 4.14). The linear Casson model cannot accurately describe the flow of chocolate over the entire shear rate ranges used in either the Brabender or Carri-Med instruments.

The ranges in viscosity and yield stress values obtained using different viscometers were comparable to published results (Steiner, 1958). As well, in collaborative studies (Steiner, 1972; Prentice and Huber, 1981) where standard chocolate samples were distributed among different laboratories and tested with different rotational instruments (using coaxial cylinder fixtures), the coefficient of variation in measured yield values was as high as 23%. The variation coefficients for yield values, obtained with the three rotational instruments used in this investigation, were 20.8, 18.5, 40.2 and 23.3% for HMC, HSS, H1 and H2, respectively.

A second experiment was conducted using samples H1 and H2 and estimating yield values from data measured over a 12 and 30 minute programmed run. The yield estimates are listed in Table 4.15 and an analysis of variance (Table 4.16) indicated that there was a significant difference in yield values measured over these two run times and a significant run x sample interaction. The yield values for sample H1 were significanlty lower when the sample was sheared for 30 minutes as compared to the yield values obtained when the sample was sheared for 12 minutes.

It is apparent that the Casson flow parameters for chocolate using the Casson flow equation depend on the accuracy of the measured flow data and the rotational instrument used. As well, the use of model equations, to estimate yield stress, may not be very

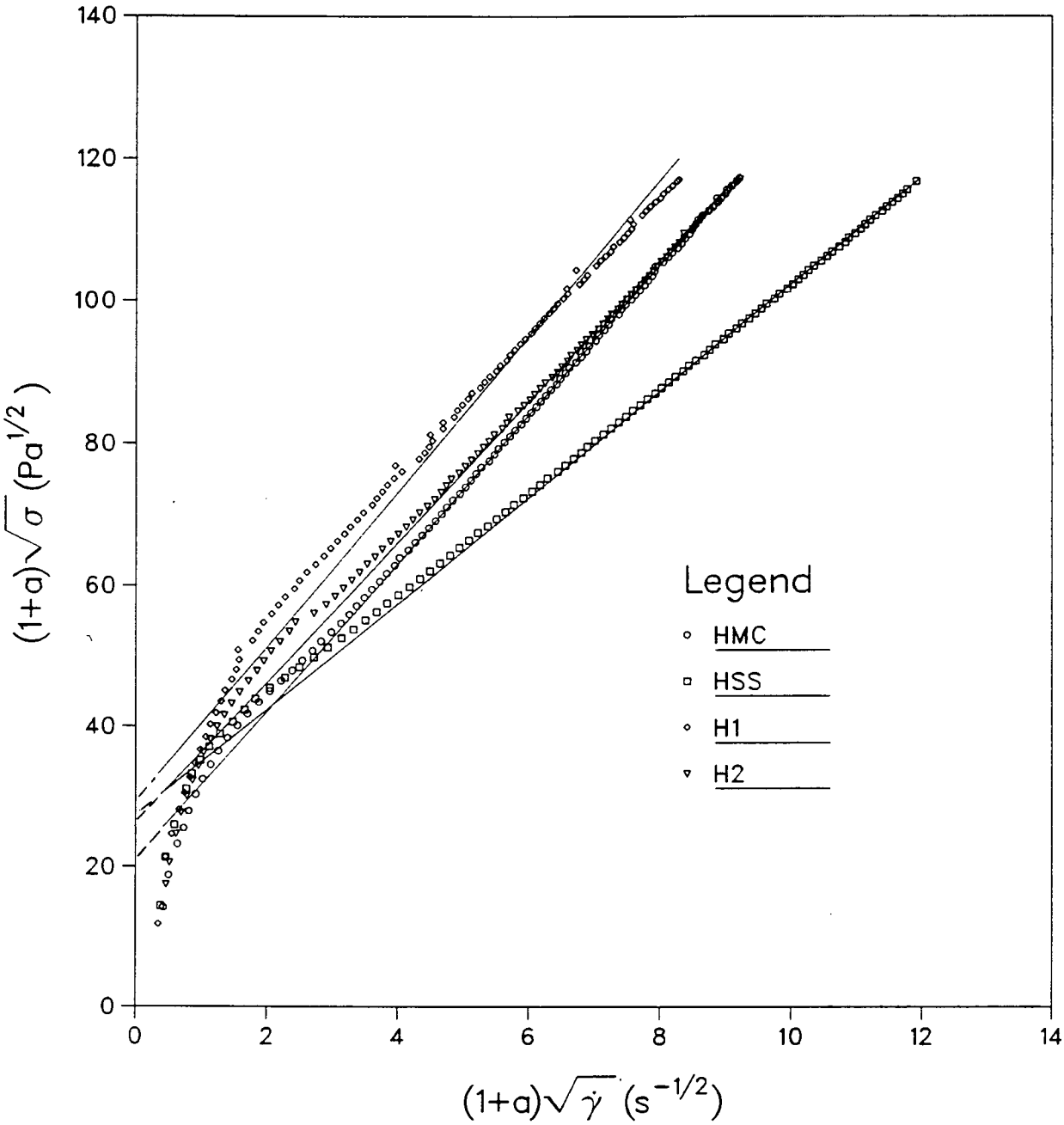

Figure 4.10: Casson flow curves of chocolate samples at 40° C obtained with the Carri-Med rheometer using coaxial cylinder fixture 5222.

Table 4.14: Mean Casson yield stress estimates for chocolate samples at 40°C recalculated over the linear portion of the rheograms obtained with the Carri-Med rheometer using coaxial cylinder fixture 5222.

Sample	Yield Stress σ_{ca}, (Pa)	Coefficient of Determination, r^2
HMC	13.9 (11.4)†	0.993 (n=360)
HSS	23.8 (3.87)	0.983 (n=358)
H1	32.0 (1.44)	0.993 (n=340)
H2	23.7 (9.76)	0.991 (n=349)

† - Coefficient of variation (%)

representative of the true physical yield property of the sample (Nguyen and Boger, 1983; Rao and Cooley, 1983).

Table 4.15: Casson yield stress estimates for chocolate samples H1 and H2 at 40°C for two run times obtained with the Carri-Med rheometer using coaxial cylinder fixture 5222.

Sample	Run Time (min)	Casson Yield σ_{ca}, (Pa)	Coefficient of Determination, r^2
H1	12	29.1 (4.73)†	.983 (n=386)
	30	20.6 (8.83)	.969 (n=389)
H2	12	9.94 (2.34)	.995 (n=381)
	30	9.49 (3.10)	.994 (n=393)

†- Coefficient of variation (%)

Table 4.16: Analysis of variance for Casson yield stress of chocolate samples at 40°C for two run times obtained with the Carri-Med rheometer using coaxial cylinder fixture 5222.

Source of Variation	df	Mean Square	F-Ratio
Sample	3	686.89	186.55 **
Error	4	3.6821	
Run Time	1	59.981	182.87 **
Interaction			
Run x Sample	1	48.410	147.60 **
Error	4	0.32799	

** - significant at $p<0.01$

4.4 STRESS RELAXATION METHOD

The results obtained with the stress relaxation methods are given in Table 4.17. Residual stress remaining in the material after shearing was stopped provided direct experimental evidence that a yield stress was present in the time frame of the experiment (Tiu and Boger, 1974).

The small yield stress values obtained could be interpreted two ways. Firstly, these values could be thought to represent the true yield stress of the samples tested. The flow curves obtained using both the Brabender and Carri-Med rheometers showed a marked curvature towards the abscissa. Since a straight line was fitted to the curved data, the intercept could be higher than if a smooth curve were to be drawn and extended to the y-axis. Accordingly, the calculated yield value of the material could therefore occur at much higher shear stresses than if the values were obtained by curvilinear extrapolation. A second interpretation, is that the low values measured were an artifact of the experiment and do not provide a meaningful estimate of the yield stress of the samples.

It is noteworthy that accuracy was not greatly improved in that, in general, coefficients of variation were higher for direct estimation of yield stress by the Stress Relaxation Method as compared to the indirect method of extrapolating flow data to zero shear rate. As well, although this residual stress method was simple, there was no great time savings in conducting this experiment. The samples had to be pre-sheared for a longer period of time (30 minutes) in order to reach an equilibrium state and, as well, several rotational speeds and relaxation periods were performed. When this procedure was shortened by using only one rotational speed, greater variation in the data was observed as shown in Table 4.17. As well, yield values were higher for the single point measurements as compared to multiple measurements made at three rotational speeds. It may be that the values measured were dependent on both shear rate and/or the test procedure used.

Table 4.17: Yield stress estimates for chocolate samples at 40°C using the Stress Relaxation Method and the Brabender viscometer with coaxial cylinder fixtures A1 and A2.

Method	Cylindrical Fixture	Yield Stress (Pa) HMC	HSS	H1	H2
Single measurement	A2	4.42 (17.3)†	4.09 (21.0)	11.1 (6.48)	5.43 (11.1)
	A1	4.23 (22.7)	4.31 (7.45)	15.8 (28.0)	6.04 (28.1)
Multiple measurements	A2	1.74 (21.5)	2.85 (14.9)	8.59 (8.07)	2.53 (10.3)
	A1	2.38 (15.0)	4.49 (11.0)	9.16 (16.3)	3.80 (10.2)

†- Coefficient of variation (%)

Robinson-Lang and Rha, 1981, and Nguyen and Boger, 1983, found this method to be acceptable for the measurement of yield stress in low and moderately concentrated clay suspensions. However, Nguyen and Boger (1983) found that in highly concentrated suspensions (greater than 60% solids by weight) slip effects and a nonuniform shear distribution contributed to poor reproducibility. As well, low recorded yield stress values for wheat starch dispersions following stress relaxation were reportedly due to slip effects (Navickis and Bagley, 1983). Chocolate melts are highly concentrated dispersions and it is possible that slip effects were occuring, resulting in lower recorded yield values.

In a collaborative study (Prentice and Huber, 1983) in which yield stress was estimated using the Casson equation, one laboratory, using cone and plate fixtures, allowed the sample to relax after each measurement. The residual stress or yield stress fell to a steady value independent of shear rate, but noted that the measured values were also

lower in magnitude than yield values obtained by extrapolation of Casson steady flow data to zero shear rate. Apart from possible slip effects, another problem in using this method is that the structure of the test material is disrupted before yield stress is measured. Stress relaxation may be an appropriate method for measuring the yield stress of molten chocolate in cases where structure of a sheared sample is important.

4.5 VANE FIXTURE METHOD

The vane fixture method was found to be applicable for direct determination of the yield stress of the four chocolate samples tested. The five vane fixtures, E, F, G, K and O were used to measure start-up torque overshoot values from which were derived estimates of the yield stress of the molten chocolate test samples. Yield stress was estimated from the raw data using three different analyses; the Single Vane Method (Keentok, 1982; Nguyen and Boger, 1983) and Multiple Vane Methods I and II (Nguyen and Boger, 1985).

4.5.1 Single Vane Method

Peak torque values were obtained by measuring the maximum torque at the start-up of vane rotation after the 15 minute pre-shear period. Low rotational speeds of 0.064, 0.120 and 0.224 rpm were used and single measurements were taken using each vane fixture. Yield stress estimates were obtained from the following relationship:

$$\sigma_y = 2T_m/[\pi D^2(H + D/3)] \tag{4.12}$$

where D and H are the diameter and height of the vane fixture, T_m is the maximum torque measured and σ_y is the calculated yield value. Table 4.18 shows the yield stress estimates determined for the four chocolate samples using single measurements taken from each vane fixture at three different speeds.

Table 4.18: Yield stress estimates for chocolate samples at 40°C using the Single Vane Method.

Sample	Rotational Speed (rpm)	Yield Stress (Pa)					Coefficient of Variation (%)
		E	F	G	K	O	
HMC	0.064	31.3	30.4	29.9	31.5	29.0	3.98
	0.120	32.8	32.9	30.2	33.0	30.0	5.45
	0.224	33.4	32.7	31.8	32.4	31.1	3.56
HSS	0.064	39.7	35.6	36.8	38.5	44.8	8.63
	0.120	42.8	37.0	38.8	39.7	44.3	7.71
	0.224	44.5	39.2	40.4	40.0	47.6	8.70
H1	0.064	70.5	109	68.0	66.5	61.1	23.45
	0.120	68.8	107	65.4	65.3	63.5	23.23
	0.224	71.9	109	66.9	66.5	65.1	22.71
H2	0.064	29.0	29.5	30.7	32.4	31.4	6.72
	0.120	30.9	31.2	30.4	36.2	31.8	8.57
	0.224	31.9	32.1	31.7	35.6	34.9	6.92

A split plot analysis was carried out to determine if there were any significant differences between vane fixtures as well as rotational speeds. The results of the analysis of variance using the BMDP:2V statistical software are given in Table 4.19. As shown, the rotational speeds (rpm) used had a significant ($p<0.01$) influence on the yield stress values obtained.

In concentrated clay suspensions, yield values measured using vane fixtures were relatively constant over rotational speeds ranging from 0.1 to 8.0 rpm, but increased at speeds greater than 8.0 rpm (Nguyen and Boger, 1983). In preliminary testing, peak torque values measured using the vanes increased significantly when rotational speeds greater than 0.8 rpm were used. Also, when measuring the yield point of a material, it would be better to use very low speeds. For these reasons, low speeds were used in the test procedure, but still lower speeds may be necessary for optimal results; however, the Brabender viscometer is not capable of applying slower speeds.

Nguyen and Boger also recommended that the diameter of the cup and the depth of the suspension in the cup be at least twice as large as the diameter and height of the vane in order to minimize boundary effects. In this investigation, vanes E, F and G, which had vane blade heights of 4.0 cm, were chosen according to these criteria. In addition, vanes K and O, which had vane blade heights of 5.5 and 7.0 cm, respectively, were used although the depth of the molten chocolate in the cup was not twice that of the height of the immersed vane. However, no significant difference was found for the different sized vanes used. The material itself may govern what the limiting dimensions of the vane(s) and cup fixtures might be.

The coefficients of variation for yield values measured using the five vane fixtures were below 10% for samples HMC, HSS and H2 (Table 4.18). The high variation in results for sample H1 is due to high peak torque values measured using vane F.

In an attempt to eliminate the effect of start-up speed on the estimated value of the

Table 4.19: Split plot analysis of variance for estimates of yield stress in chocolate samples at 40°C using the Single Vane Method.

Source of Variation	df	Mean Square	F-Ratio
Sample	7	548.13E01	20.47 **
Vane	4	418.32	1.57 ns
Error	28	267.76	
Speed	2	46.829	33.35 **
Interactions			
Speed x Sample	14	2.8797	2.05 *
Speed x Vane	8	2.2798	1.62 ns
Error	56	1.4043	

* - significant at $p<0.05$ ** - significant at $p<0.01$ ns - not significant ($p>0.05$)

Table 4.20: Yield stress estimates for chocolate samples at 40°C from extrapolating mean yield stress values for vanes at three start-up speeds to zero rpm.

Sample	Rotational Speed (rpm)	Mean Yield Stress (Pa)	Extrapolated Yield Stress (Pa)	Standard Error Estimate of Y	Coefficient of Determination r^2
HMC	0.064	30.4	28.6	1.46	0.213 (n=30)
	0.120	31.8			
	0.224	32.3			
HSS	0.064	39.1	35.4	3.52	0.132 (n=30)
	0.120	40.5			
	0.224	42.3			
H1	0.064	66.5	64.7	5.61	0.008 (n=24)
	0.120	65.7			
	0.224	67.6			
H2	0.064	30.6	27.7	2.48	0.166 (n=30)
	0.120	32.1			
	0.224	33.2			

yield point, the yield stress was calculated by extrapolation of data gathered at finite rotational speeds, back to zero rpm (Tung et al., 1990). The data were successfully fitted by the following equation,

$$\sigma_y = a\sqrt{rpm} + \sigma_{y_0} \tag{4.13}$$

Yield stress (σ_{y_0}) values estimated by this procedure (Figure 4.11) would presumably be independent of rotational speed employed. The values are listed in Table 4.20. Vane F data for sample H1 were omitted in this analysis. The standard error estimates reflect the accuracy of the yield values obtained for the chocolate samples using this method.

Yield stress values calculated at zero rpm were slightly lower than the mean yield values obtained at 0.064, 0.120 and 0.224 rpm.

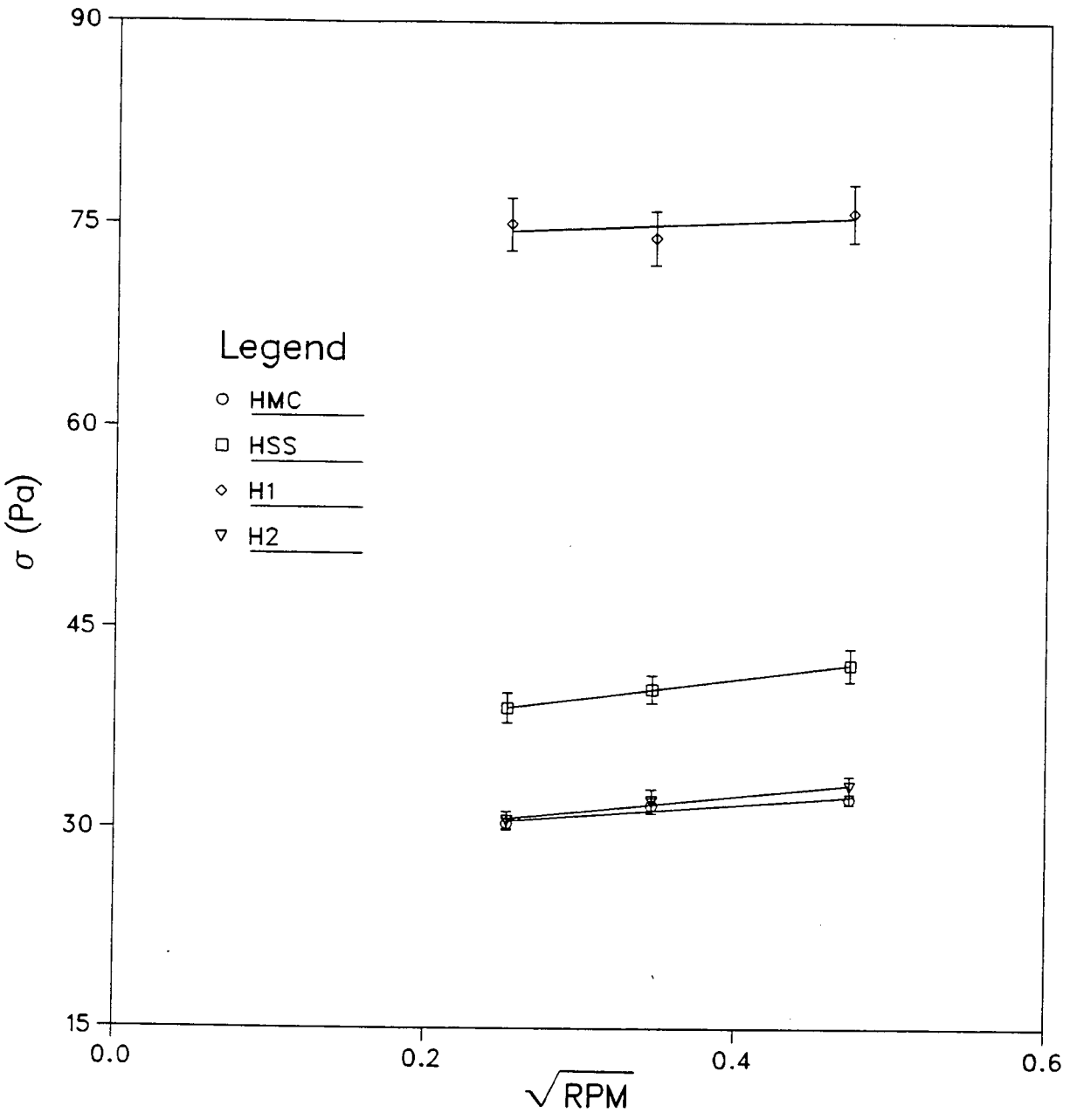

Figure 4.11: Yield stress estimated at zero rpm for the chocolate samples at 40°C using mean yield values obtained from the five vane fixtures.

4.5.2 Multiple Vane Method I

This method utilized Equation 2.11 as described previously in Chapter 2. By plotting $2T_m/\pi D^3$ as a function of the vane length to diameter ratio (H/D), the yield stress can be determined directly from the slope of the graph.

The vane fixture data were analyzed according to this method using vanes E, F, G, K and O with H/D varying from 1.6 to 2.8. A linear regression test for equality of lines using the BMDP:1R statistical computer program showed there was no significant difference ($p>0.05$) between duplicates tested. The duplicates were pooled and the data plotted for each chocolate sample at each of the three rotational speeds used. The results obtained from the analysis are listed in Table 4.21.

For chocolate samples HMC, HSS and H2, the linearity of plots in Figure 4.12 confirms the validity of this method for the set of vane fixtures used. However, this analysis was not adequate for calculating the yield value of H1 as shown by the plotted data in Figure 4.12 for this sample. It appears that measurements obtained using vanes E and F were responsible for the scatter in the plotted data. When these data points were removed the recalculated yield values were 49.9, 60.4 and 62.2 Pa for speeds of 0.064, 0.120 and 0.224 rpm, respectively, which compared more closely with the single point measurements. These vanes were the smallest in both diameter and height of the series of vanes used in this investigation. It may be that small vanes should not be used to test highly viscous chocolate melts.

Table 4.21 also lists the values for m, an empirical parameter describing the stress distribution at either end of the vane fixture and should vary little about zero. The m values for samples H1 and HSS, as well as the m value obtained at the highest test speed for sample H2, were large, and therefore, some error in calculating the yield values would result. In fact, the yield values obtained for these samples do not compare with yield

Table 4.21: Yield stress estimates for chocolate samples at 40°C using Method I for analyzing vane fixture data.

Sample	Rotational Speed (rpm)	Yield Stress σ_y, (Pa)	m	Coefficient of Determination, r^2 n=10
HMC	0.064	29.5	-0.60	0.947
	0.120	31.2	-0.37	0.906
	0.224	32.1	-0.10	0.959
HSS	0.064	55.2	-5.49	0.937
	0.120	54.8	-6.08	0.950
	0.224	59.4	-5.56	0.931
H1	0.064	34.0	-2.70	0.125
	0.120	40.8	-2.58	0.175
	0.224	44.4	-2.53	0.197
H2	0.064	30.1	-0.32	0.848
	0.120	32.3	+0.16	0.793
	0.224	37.0	+9.41	0.871

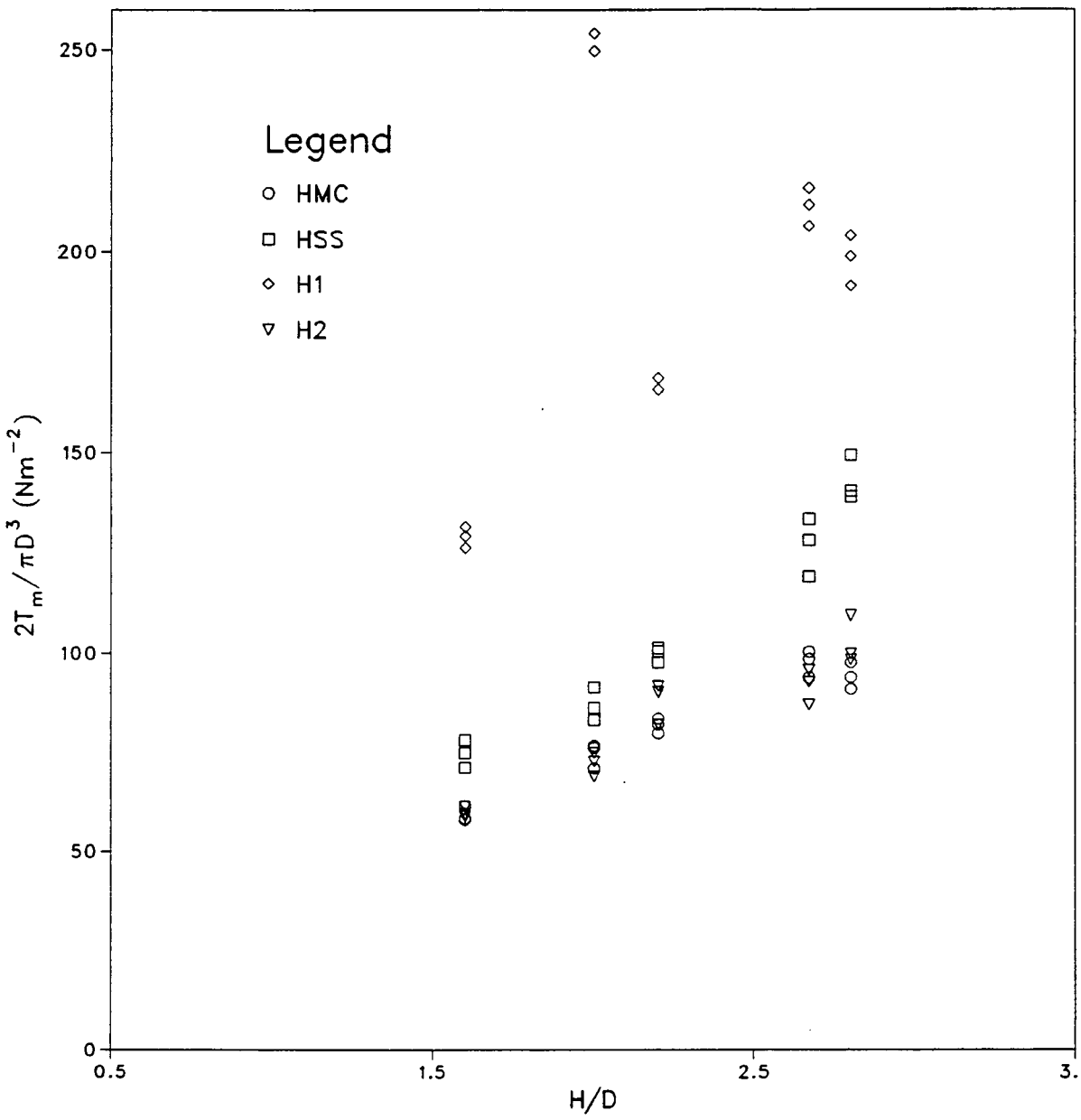

Figure 4.12: Plot of $2T_m/\pi D^3$ versus H/D (Method I) for estimating yield stress of chocolate samples at 40°C using vane fixtures E, F, G, K and O.

Table 4.22: Analysis of variance in yield stress estimates derived at various rotational speeds in chocolate samples at 40°C using multiple vane fixture data analyzed by Method I.

Source of Variation	df	Mean Square	F-Ratio
Sample	3	625.29	84.45 *
Speed	2	42.389	5.73 *
Error	6	7.4041	

* - significant at $p<0.05$

values estimated using the Single Vane Method. For chocolate samples HMC and H2 (at the two lower speeds), m ranged from -0.60 to -0.10 and the corresponding yield values were comparable to those obtained using single vane measurements. A uniform shear stress distribution over the end surfaces of the vane fixture was confirmed experimentally for clay suspensions (Nguyen and Boger, 1985; James et al., 1987), but could not be confirmed for two of the four chocolate samples tested in this investigation, thus, some error in estimating the yield value for these samples could result.

In order to test for possible differences between rotational speeds, a two-way analysis of variance (ANOVA) was conducted using the BMDP:2V statistical software. Analysis of variance results in Table 4.22 indicated that rotational speed significantly affected the derived yield stress, but this effect was only marginally significant ($p=0.0407$).

4.5.3 Multiple Vane Method II

Experimental data for vane fixtures, G, K and O were analyzed using the second method proposed by Nguyen and Boger (1985). These vanes had a diameter of 2.5 cm and ranged in height from 4.0 to 5.5 and 7.0 cm for fixtures G, K and O, respectively. By using a series of vane fixtures which have the same diameter but different heights, the shear stress distribution at either end of the vane fixture did not have to be considered. The yield stress was then estimated from the slope of the peak torque versus vane fixture height function using the following equation:

$$\sigma_y = 2slope/\pi D^2 \tag{4.14}$$

A linear relationship was found between the peak torque and vane fixture height (Figure 4.13) for each of the samples tested. This supports the validity of assumptions made in analyzing the vane fixture data by Method II. Yield stress values derived by this procedure are listed in Table 4.23.

For graphical purposes, data from the duplicate measurements were pooled as well as the peak torque data obtained over the three rotational speeds used. A test for equality of lines showed there were no significant differences ($p>0.05$) between duplicates. The effect of start-up speed was analyzed in a two-way analysis of variance and showed no significant difference ($p>0.05$, Table 4.24).

Yield values estimated for samples HMC and H2 were comparable among the three vane methods used. For sample HSS, Methods I and II gave comparable estimates for yield stress, but these values were not comparable with the single point measurements. For sample H1, the yield values were somewhat similar between the Single Vane Method and Method II, but were much lower when Method I was used. For HSS and H1, the m values would indicate that the Method I analysis and, therefore, the torque balance equation used to estimate yield stress for single point measurements for these samples

Table 4.23: Yield stress estimates for chocolate samples at 40°C using Method II for analyzing vane fixture data.

Sample	Rotational Speed (rpm)	Yield Stress σ_y, (Pa)	Coefficient of Determination, r^2 n=6
HMC	0.064	27.5	0.946
	0.120	29.6	0.916
	0.224	30.1	0.973
HSS	0.064	57.7	0.967
	0.120	53.3	0.954
	0.224	59.3	0.944
H1	0.064	50.0	0.911
	0.120	60.3	0.927
	0.224	62.2	0.932
H2	0.064	32.4	0.956
	0.120	34.1	0.871
	0.224	40.2	0.957

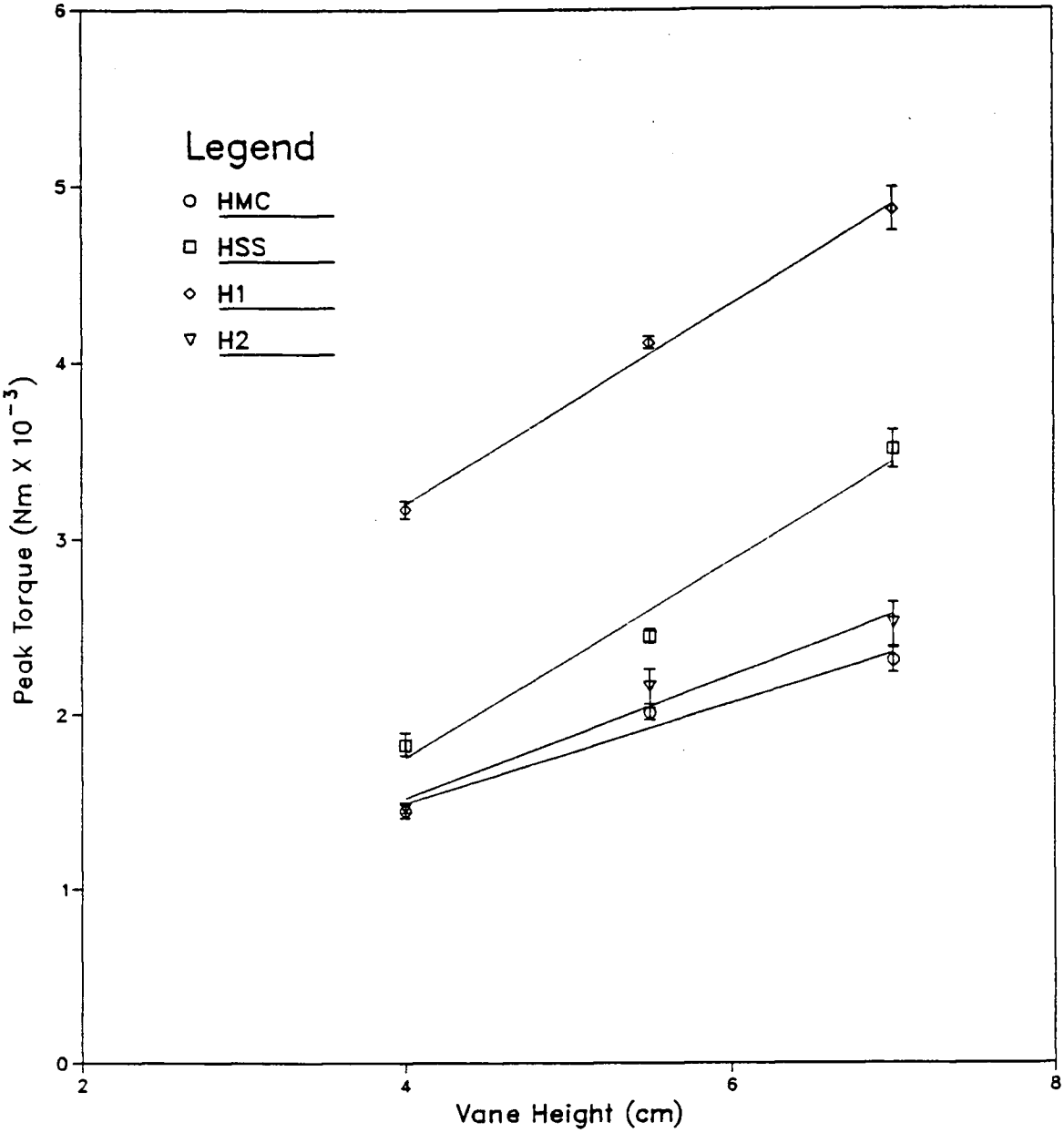

Figure 4.13: Plot of peak torque versus vane height (Method II) for estimating yield stress of chocolate samples at 40°C using vane fixtures G, K and O.

Table 4.24: Analysis of variance for yield stress estimates derived at various rotational speeds for chocolate samples at 40°C using multiple vane fixture data analyzed by Method II.

Source of Variation	df	Mean Square	F-Ratio
Sample	3	636.89	54.80 **
Speed	2	37.392	3.22 ns
Error	6	11.622	

** - significant at $p<0.01$ ns - not significant ($p>0.05$)

would result in some error.

H1 and HSS had the highest yield stress values of the four test samples and, therefore, it is possible that larger vane fixtures would be more suitable for testing very thick samples. For example, vane E and F data, using the Method I analysis, appear to be responsible for the variability found in the yield values measured for H1. This sample proved difficult to characterize using both indirect and direct methods. However, a better estimate of the yield stress value may be made using a vane fixture rather than a coaxial cylinder fixture where slip effects can cause significant error. In cases where single point measurements are questionable, Method II could be used to verify the yield estimates where data are obtained using at least a minimum of three vane fixtures.

In general, yield stress values obtained using the vane methods were 1.5 to 2.5 times higher than the Casson yield stress estimates. Higher yield values obtained using the vane methods as compared to yield values obtained using the Casson model equation have been reported by other researchers (Keentok, 1982; James et al., 1987; Tung et al., 1990). As well, other direct methods used to measure the yield stress of starch suspensions, butter

and mayonnaise have resulted in higher comparative yield values than those determined by indirect methods (Elliot and Green, 1972; Elliot and Ganz, 1977; Navickis and Bagley, 1983).

It has been suggested that the discrepancy in the yield values measured using both direct and indirect methods may reflect the way in which the yield point was measured. For example, measurements using the vane fixture are made under virtually static conditions. When model equations are used to estimate the yield stress, the equation is fitted to shear stress-shear rate flow data measured over a range of shear rates. Researchers have used the terms *static* yield stress and *dynamic* yield stress as a means of distinguishing between values measured under these two conditions (Cheng, 1978; Keentok, 1982; Cheng, 1986).

Chapter 5

CONCLUSIONS

This study investigated several methodologies that could be used to estimate the yield stress of molten chocolate. The conventional method used is the OICC method, based on obtaining steady flow viscometric data and extrapolating the fitted model to zero shear rate. The accuracy of this method was checked using flow data obtained with three different rotational instruments. In addition, four alternative methods were used to measure the yield stress value directly. The chocolate test samples included two types of commercial chocolate samples and two experimental chocolate samples; all were obtained from the Hershey Chocolate Company.

The composition of the samples was determined by proximate and sucrose analyses. As well, the mean particle size and distribution of sizes contained in the samples was determined. A multivariate analysis of variance indicated a significant difference ($p<0.01$) in composition among samples tested for ash, moisture, protein, carbohydrate and sucrose content, and a significant difference ($p<0.05$) for fat content. The mean particle sizes were found to be 5.73, 6.27, 6.98 and 7.15 μm for samples HSS, H1, HMC and H2, respectively. The largest population of particles was found to be in the size range of 4.0 to 5.0 μm.

The yield stress of four chocolate samples at 40°C was measured indirectly using the Casson flow model and directly using the Stress Relaxation Method, the Single Vane Method and Multiple Vane Methods I and II. The Casson flow model was fitted to shear stress-shear rate data to obtain an estimate of the yield value by extrapolation. Flow data

were obtained with the Brookfield HAT viscometer, the Brabender Rheotron viscometer and the Carri-Med Controlled Stress Rheometer. Mean Casson yield stress values for the four chocolate samples ranged from 9.38 to 15.7 Pa for HMC, from 19.8 to 29.3 Pa for HSS, from 9.59 to 30.4 Pa for H1 and from 10.6 to 19.9 Pa for H2 as determined using the three instruments. Samples H1 and HSS had the highest yield stress values as well as the highest concentration of small particles of the four chocolates tested. Coefficients of variation for yield values from flow data obtained from the three different instruments were approximately 20% for samples HMC, HSS, and H2 and 40% for sample H1.

The Casson flow model fitted the flow data for chocolate samples HMC, HSS and H2 obtained from the Brookfield viscometer. However, a deviation from linearity was apparent when this model equation was fitted to the flow data for H1, and, thereby, some error in calculating the yield value resulted. Also, sample H1 was very thick and it was possible that slippage took place within the annular gap, which would lead to a lower estimate of yield stress than was expected.

Deviation from linearity below approximately 0.5 s^{-1} was apparent when the Casson equation was fitted to the flow data obtained with both the Brabender and Carri-Med instruments. The Casson equation did not accurately describe the flow properties of the molten chocolate samples over the shear rate range tested, therefore, it was difficult to estimate the exact yield point of the sample. Yield values obtained from recalculation over the linear data points were higher. Further uncertainty was contributed by the fact that yield and viscosity values determined from flow data obtained with the Brabender using two coaxial cylinder fixtures of different gap widths were significantly different ($p<0.05$). Also, there was a significant fixture by sample effect ($p<0.05$).

Using the Carri-Med rheometer, viscosity estimated from consecutive flow runs were significantly different ($p<0.05$). In a second experiment, where samples H1 and H2 were sheared over two different run times of 12 and 30 minutes, resulted in significantly

different yield values measured for sample H1, and a significant run by sample interaction ($p<0.01$). The observed variability in the Casson flow parameters over the three different instruments used lends some uncertainty as to the accuracy of this method.

Alternative methods of measuring the yield stress of molten chocolate were investigated. Yield values measured using the Stress Relaxation Method were very low and were believed to be an artifact of the measuring fixture and instrument. Low yield values have been reported by other researchers when testing very thick fluids by this method. However, residual stress measurements could be used to study the structural recovery of materials that have undergone shear.

The direct measurement of yield stress using vane fixtures was also investigated. A series of five vane fixtures of varying dimensions was used to measure peak torque values on sudden start-up obtained with the Brabender viscometer. Using the Single Vane Method, single point measurements were made at three different rotational speeds. An analysis of variance indicated a significant difference ($p<0.01$) in yield values measured using speeds of 0.064, 0.120 and 0.224 rpm. The speed by sample interaction was also significant at the $p<0.05$ level. There was no significant difference in yield values measured using different vane fixtures.

The speed effect was marginally significant ($p<0.04$) when the peak torque data were analyzed using Method I, but was not a significant factor in Method II. Method I appeared to give valid estimates of the yield values for chocolate samples HMC, HSS and H2, but not for sample H1. As well, the values for the constant, m, used in this analysis, were large for samples HSS and H1 and, therefore, the assumption of a uniform shear stress distribution over the ends of the vane was not valid. It is recommended that Multiple Vane Method II be used instead of Method I because it is not necessary to make any assumptions as to the nature of the stress distribution over the ends of the vane.

Method II required more time to calculate a yield value than did the Single Vane

Method, but considerably less time was required to estimate yield stress by these methods as compared to the conventional OICC method using the Casson flow model. As well, the use of vane fixtures offers several other advantages. Problems with sample slip were not apparent, the immersion of the vane into the sample is far less disruptive than when using cylindrical fixtures and the level of precision required when using narrow gap coaxial cylinder fixtures is not necessary with vane fixtures.

The disadvantage of using vane fixtures was that more sample volume was required for testing. As well, a viscosity estimate cannot be obtained because, under steady shear conditions, the flow about the vane blades would be difficult to characterize.

The vane methods appear to provide an accurate assessment of the yield value of molten chocolate. Although values are 1.5 to 2.5 times higher than the Casson yield stress values, this may be explained by the differences in which the yield point was measured. It has been suggested by other researchers that the terminology for the yield stress value be further clarified to include the terms, *static* yield stress and *dynamic* yield stress where yield is measured under static conditions or measured from steady shearing flow.

Further investigation of the vane method is recommended. The speed effect evidenced with the Brabender viscometer may not be evident in other constant shear rotational instruments where the inertial effects of the fixture and torque measuring system may differ. Also, the speed effect would be eliminated if a controlled stress rheometer was used. Additional vane fixtures might also be used to best determine the types and sizes of fixtures most suitable for testing molten chocolate. If further investigation of the vane methods proves satisfactory, this method of estimating the yield stress of molten chocolate could be used for quality control purposes.

LITERATURE CITED

[1] Abbink, J. 1984. Shelflife of compounded chocolate. Confect. Manuf. and Market. 21(10):16.

[2] AOAC. 1984. Official Methods of Analysis, 14th ed. Association of Official Analytical Chemists, Washington, DC.

[3] Balmaceda, E., Huang, F. and Rha, C.K. 1973. Rheological properties of hydrocolloids. J. Food Sci. 38:1169.

[4] Banford, H.F., Gardiner, K.J., Howat, G.R. and Thomson, A.F. 1970. The use of polyglycerol polyricinoleate in chocolate. Confect. Prod. 36:359.

[5] Barbosa-Canovas, G.V. and Peleg, M. 1983. Flow parameters of selected commercial semi-liquid food products. J. Text. Stud. 14:213.

[6] Brookfield Engineering Laboratories Inc. 1985. When Viscosity is Measured. Stoughton, MA.

[7] Brownsey, G.J. 1988. Commercial rotational instruments. In Rheological Measurement, A.A. Collyer and D.W. Clegg (Eds.) p. 405. Elsevier Applied Science Publishers Ltd., London, UK.

[8] Carri-Med Ltd. Instruction Handbook for the Carri-Med Controlled Stress Rheometer. Dorking, UK.

[9] Casson, N. 1959. A flow equation for pigmented-oil suspensions of the printing ink type. In Rheology of Disperse Systems, C.C. Mill (Ed.) p. 82. Pergamon Press, New York, NY.

[10] Charm, S.E. 1963. The direct determination of shear stress-shear rate behavior of foods in the presence of a yield stress. J. Food Sci. 28(1):107.

[11] Cheng, D.C-H. 1978. On Bingham plastic fluids: theory and practice. Br. Soc. Rheol. Bull. 21:60.

[12] Cheng, D.C-H. 1986. Yield Stress: A time dependent property and how to measure it. Rheol. Acta. 25:542.

[13] Chevalley, J. 1975. Rheology of chocolate. J. Text. Stud. 6:177.

[14] Cloud, J.E. and Clark, P.E. 1985. Alternatives to the power-law fluid model for cross-linked fluids. Soc. Petrol. Eng. J. 25:935.

[15] Cockinos, C. 1985. Developments in chocolate manufacturing. Manuf. Confect. 65(2)55.

[16] Concon, J.M. and Soltess, D. 1973. Rapid micro-Kjeldahl digestion of cereal grains and other biological materials. Analytical Biochem. 53:35.

[17] C.W. Brabender Instruments Inc. The Brabender Rheotron Instruction Manual. South Hackensack, NJ.

[18] Darby, R. 1985. Couette viscometer data reduction for materials with a yield stress. J. Rheol. 29(4):369.

[19] Davis, S.S., Deer, J.J. and Warburton, B. 1968. A concentric cylinder air turbine viscometer. J. Sci. Instr. 1:933.

[20] De Kee, D., Turcotte, G. and Fildey, K. 1980. New method for the determination of yield stress. J. Text. Stud. 10:281.

[21] Dervisoglu, M. and Kokini, J.L. 1986. Steady shear rheology and fluid mechanics of four semi-solid foods. J. Food Sci. 51(3):541.

[22] Dixon, W.J. 1985. BMDP Statistical Software. University of California Press, Berkeley, CA.

[23] Duck, W.N. 1965. A rapid method for calculation of Casson flow values of chocolate. Manuf. Confect. 45(5):33.

[24] Elliott, J.H. and Ganz, A.J. 1977. Salad dressings - preliminary rheological characterization. J. Text. Stud. 8:359.

[25] Elliott, J.H. and Green, G.E. 1972. Modification of food characteristics with cellulose hydrocolloids. II. The modified Bingham body - a useful rheological model. J. Text. Stud. 3:194.

[26] Franck, A.J.P. 1985. A rheometer for characterizing polymer melts and suspensions in shear creep and recovery experiments. J. Rheol. 29(6):833.

[27] Hanks, R.W. 1983. Couette viscometry of Casson fluids. J. Rheol. 27(1):1.

[28] Heathcock, J.F. 1985. Characterization of milk proteins in confectionery products. Food Microstructure. 4(1):17.

[29] Heimann, W. and Fincke, A. 1962a. Rheometry of chocolate - the flow equation of Casson and its application to rheometry of chocolate. Z Lebensm. Untersuch. Forsch. 117:93.

[30] Heimann, W. and Fincke, A. 1962b. Measuring the flow limits and their calculation from the Casson equation. Z Lebensm. Untersuch. Forsch. 117:225.

[31] Heimann, W. and Fincke, A. 1962c. Application of a modified Casson equation to milk chocolates and cocoa pastes. Z. Lebensm. Untersuch. Forsch. 117:297.

[32] Heimann, W. and Fincke, A. 1962d. Temperature dependence of the flow behavior of molten chocolate. Z. Lebensm. Untersuch. Forsch. 117:301.

[33] Howard, D.W. 1969a. Adapted instrument measures Casson values. Candy Ind. 133(8):21.

[34] Howard, D.W. 1969b. Brookfield develops reliable measurement of chocolate viscosity. Manuf. Confect. 49(10):48.

[35] Hunter, R.J. and Nicol, S.K. 1968. The dependence of plastic flow behavior of clay suspensions on surface properties. J. Colloid. and Interface Sci. 28(2):250.

[36] James, A.E., Williams, D.J.A. and Williams, P.R. 1987. Direct measurement of static yield properties of cohesive suspensions. Rheol. Acta. 26(5):437.

[37] Kaletunc-Gencer, G. and Peleg, M. 1984. Digitizer aided determination of yield stress in semi-liquid foods. J. Food Sci. 49(6):1620.

[38] Keentok, M. 1982. The measurement of the yield stress of liquids. Rheol. Acta. 21:325.

[39] Kiljanski, T. 1989. A method for correction of the wall-slip effect in a Couette rheometer. Rheol. Acta. 28:61.

[40] Kleinert, J. 1976. Rheology of chocolate. In Rheology and Texture in Food Quality, J.M. deMan, P.W. Voisey, V.F. Rasper and D.W. Stanley (Eds.) p.445. AVI Publishing Co. Inc., Westport, CT.

[41] Kleinert, J. 1982a. Cyclo-TRG measurements I. Rev. Choc., Confect. and Bakery. 7(2):4.

[42] Kleinert, J. 1982b. Cyclo-TRG measurements II. Rev. Choc., Confect. and Bakery. 7(2):4.

[43] Kleinert, J. 1982c. Cyclo-TRG measurements III. Rev. Choc., Confect. and Bakery. 7(3):3.

[44] Krieger, I.M. 1968. Shear rate in the couette viscometer. Trans. Soc. Rheol. 12:5.

[45] Kuster, W. 1985. Efficient use of five-roll refiner in producing chocolates and other fatty mixtures. Manuf. Confect. 65(6):55.

[46] Lang, E.R. and Rha C.K. 1981. Determination of the yield stress of hydrocolloid dispersions. J. Text. Stud. 12:47.

[47] Levine, L. 1987. An introduction to the measurement of viscosity. Viscous Products. p. 14.

[48] Malm, M. 1967a. Interrelation between Casson values and other properties of chocolate. Manuf. Confect. 47(5):63.

[49] Malm, M. 1967b. More refining raises chocolate yield value. Candy Ind. 129(8):21.

[50] Malm, M. 1968. Inter-relations between Casson values and other properties of sweet and milk chocolate. Confect. Manuf. Market. 5(2):22.

[51] Markov, E. and Tscheuschner, H.D. 1989. Instrumental texture studies n chocolate: IV. Comparison between instrumental and sensory texture studies. J. Text. Stud. 20:151.

[52] Minifie, B. (Ed.). 1980. Chocolate, Cocoa and Confectionery. AVI Publishing Co. Inc., Westport, CT.

[53] Motz, R.J. 1964. Notes on viscometry. Rev. Intern. Chocolat. 19:198.

[54] Navickis, L.L. and Bagley, E.B. 1983. Yield stresses in concentrated dispersions of closely packed, deformable gel particles. J. Rheol. 27(6):519.

[55] Nguyen, Q.D. and Boger, D.V. 1983. Yield stress measurement for concentrated suspensions. J. Rheol. 27(4):321.

[56] Nguyen, Q.D. and Boger, D.V. 1985. Direct yield stress measurement with the vane method. J. Rheol. 29(3):335.

[57] Niediek, I.E.A. 1980. The characterisation of the flow properties of melted chocolated masses. Rev. Choc., Confect. and Bakery. 5(3):3.

[58] Niediek, I.E.A. 1981. The characterisation of the flow properties of melted chocolated masses II. Rev. Choc., Confect. and Bakery. 6(2):3.

[59] Office International du Cacao et du Chocolate. 1970. 1973. Viscosity of Chocolate - determination of Casson yield value and Casson plastic viscosity. Int. Choc. Review. 28(9):223.

[60] Paredes, M.D.C., Rao, M.A. and Bourne, M.C. 1989. Rheological characterization of salad dressings 2: Effect of storage. J. Text. Stud. 20:235.

[61] Patton, T.C. 1966. A new method for the viscosity measurement of paint in the settling, sagging, leveling and penetration shear rate range of .001 to 1.0 reciprocal seconds using a cone/plate spring relaxation technique. J. Paint Technol. 38(502):656.

[62] Prentice, J.H. and Huber, D. 1981. Results of the colaborative study on measuring rheological properties of foodstuffs. In Physical Properties of Foods, R. Jowitt, F. Esher, B. Hallstrom, H.F.Th. Meffert, W.E.I. Spiess and G. Vos (Eds.) p. 123. Applied Science Publishers, London, UK.

[63] Qiu, C.G. and Rao, M.A. 1989. Effect of dispersed phase on the slip coefficient of apple sauce in a concentric cylinder viscometer. J. Text. Stud. 20:57.

[64] Rao, M.A. and Cooley, H.J. 1983. Applicability of flow models with yield for tomato concentrates. J. Food Process Eng. 6:159.

[65] Reade, M.G. 1985. Cooling processes - the natural rate of solidification of chocolate. Manuf. Confect. 65(1):59.

[66] Robbins, J.W. 1979. A quick, reliable method for measuring yield value, plastic viscosity and MacMichael viscosity of chocolate. Manuf. Confect. 59(5):38.

[67] Robbins, J.W. 1983. Methods for measuring particle size distribution of chocolate products. Candy Ind. 148(7):39.

[68] Rosen, M.R. and Foster, W.W. 1978. Approximate rheological characterization of Casson fluids - Template method for the Brookfield Synchro-lectric viscometers. J. Coatings Technol. 50(643):39.

[69] Rostagno, W., Chevalley, J. and Viret, D. 1974. Rheological properties of chocolate. First International Congress on Cocoa and Chocolate Research. 174.

[70] Rostagno, W. 1974. Rheological properties of chocolate. Dechema-monographien. 77:283.

[71] Saunders, P.R. 1968a. The flow properties of chocolate in relation to structure. Brit. Food. Manuf. Ind. Res. Assoc. Techn. Circ. No. 387.

[72] Sequine, E.S. 1986. Instrument review: Brookfield. Manuf. Confect. 66(1):49.

[73] Smith, R.E. 1982. Brookfield viscometers for determination of low-shear viscosity and leveling behavior. J. Coatings Technol. 54(694):21.

[74] Solstad, O. 1983. Viscosity properties of chocolate. Manuf. Confect. 63(8):41.

[75] Sommer, K. 1974. On the flow behavior of chocolate masses. First Intern. Cong. on Cocoa and Chocolate Res., Munich, May 8-10, p.181.

[76] Steel, R.G.D. and Torrie, J.H. 1960. Principles and Procedures of Statistics. Mcgraw-Hill Book Co. Inc., New York, NY.

[77] Steiner, E.H. 1958. A new rheological relationship to express the flow properties of melted chocolate. Brit. Food. Manuf. Ind. Res. Assoc. 13(7):290.

[78] Steiner, E.H. 1962. An investigation into the validity of the Casson relationship for melted chocolate at low rates of shear and at various temperatures. Brit. Food. Manuf. Ind. Res. Assoc. 17:150.

[79] Steiner, E.H. 1972. Melted chocolate: Measuring its viscosity. Manuf. Confect. 52(9):24.

[80] Swartzel, K.R., Hamann, D.D. and Hansen, A.P. 1980. Rheological modelling of UHT milk gels using a cone and plate creep-relaxation test. J. Food Process. Eng. 161.

[81] Tiu, C. and Boger, D.V. 1974. Complete rheological characterization of time-dependent food products. J. Text. Stud. 5:329.

[82] Tscheuschner, H.D. and Markov, E. 1986. Instrumental texture studies on chocolate: I. Methods of measurement and texture characteristics. J. Text. Stud. 17:37.

[83] Tscheuschner, H.D. and Wünsche, D. 1979. Rheological properties of chocolate masses and the influence of some factors. Ch. 3. In Food Texture and Rheology, P. Sherman (Ed.), p. 355. Academic Press, London, UK.

[84] Tung, M.A., Speers, R.A., Britt, I.J., Owen, S.R. and Wilson, L.L. 1990. Yield stress characterization of structured foods. In Engineering and Food: Volume 1. Physical Properties and Process Control, W.E.L. Spiess and H. Schubert (Eds.) p. 79. Elsevier Applied Science, London, UK.

[85] Tung, M.A. and Speers, R.A. 1986. Development of Yield Stress Measurement Methodology. Final Report. DSS File No. 01SG.97702-R-5-0679, prepared for Defence Research Establishment Suffield, Ralston, AB.

[86] Van Wazer, J.R., Lyons J.W., Kim K.Y. and Colwell, R.E. 1963. Viscosity and Flow Measurement - A Laboratory Handbook of Rheology. John Wiley and Sons Inc., New York, NY.

[87] Vocadlo, J.J. and Charles, M.E. 1971. Measurement of yield stress of fluid-like viscoplastic substances. Can. J. Chem. Eng. 49:576.

[88] Wildemuth, C.R. and Williams, M.C. 1985. A new interpretation of viscosity and yield stress in dense slurries: coal and other irregular particles. Rheol. Acta. 24:75.

[89] Yoshimura, A.S., Prud'homme, R.K., Princen, H.M. and Kiss, A.D. 1987. A comparison of techniques for measuring yield stresses. J. Rheol. 31(8):699.

[90] Yoshimura, A. and Prud'homme, R.K. 1988. Wall slip corrections for couette and parallel disk viscometers. J. Rheol. 32(1):53.

[91] Zangger, R. 1984. Rheometry of chocolate melts. Alimenta. 23(1):13.

Appendix A

LISTING OF EXPERIMENTAL FLOW DATA

Table A.25: Shear stress data (Pa) for chocolate samples at 40°C obtained with the the Brookfield HAT viscometer using coaxial cylinder fixture SC4-27/13R for steady shear tests at ascending (asc) and descending (dsc) shear rate.

Shear Rate (s^{-1})	HMC		HSS		H1		H2	
	asc	dsc	asc	dsc	asc	dsc	asc	dsc
0.340	33.0	28.5	46.9	43.8	36.0	35.0	28.2	27.2
0.850	49.2	42.6	60.5	57.1	70.8	66.0	36.7	35.7
1.70	67.0	59.8	74.0	71.8	99.6	94.8	46.9	45.6
3.40	96.3	89.4	95.6	93.6	138	133	63.3	61.3
6.80	146	144	132	130			94.5	89.1
17.0							164	163

Table A.26: Shear stress data (Pa) for chocolate samples at 40°C obtained with the Brabender Rheotron viscometer using coaxial cylinder fixture A1 and spring C for steady shear tests at ascending (asc) and descending (dsc) shear rate.

Shear Rate (s^{-1})	HMC		HSS		H1		H2	
	asc	dsc	asc	dsc	asc	dsc	asc	dsc
0.191	28.9	23.0	39.9	34.7	37.1	36.7	25.4	22.3
0.358	36.4	30.8	50.8	46.6	44.3	43.8	34.3	31.9
0.669	43.2	37.7	58.8	55.5	56.6	55.8	39.0	35.8
1.30	50.8	48.6	67.7	65.5	75.9	74.2	47.1	44.0
2.54	69.0	67.7	82.7	78.5	97.6	96.1	58.6	54.9
5.00	103	101	106	102	135	133	77.4	72.5
10.0	175	170	157	152	198	194	113	106
25.0	305	287	243	235	321	303	194	180
24.2	286	266	231	225	308	286	178	167
40.3	492	451	369	361	488	449	306	285
75.8	787	744	607	594	742	720	490	479

Table A.27: Shear stress data (Pa) for chocolate samples at 40°C obtained with the Brabender Rheotron viscometer using coaxial cylinder fixture A2 and spring C for steady shear tests at ascending (asc) and descending (dsc) shear rate.

Shear Rate (s^{-1})	HMC		HSS		H1		H2	
	asc	dsc	asc	dsc	asc	dsc	asc	dsc
0.066	18.5	14.2	27.3	23.0	27.6	28.6	22.5	20.2
0.124	25.6	21.8	39.2	34.4	36.7	38.0	29.9	28.1
0.231	31.4	27.3	44.3	39.7	51.4	51.9	34.2	32.1
0.448	35.9	33.7	52.1	49.1	69.3	67.6	37.7	35.9
0.877	45.3	42.0	58.7	55.7	85.8	80.0	43.3	41.5
1.73	59.2	58.4	71.1	68.1	107	103	52.4	50.6
3.46	89.1	87.5	93.1	89.8	149	139	70.1	67.6
8.63	147	141	127	123	219	199	102	96.0
8.38	138	136	123	120	208	193	98.2	92.9
13.9	231	217	184	178	328	289	154	142
26.2	379	345	282	274	463	433	238	225
50.8	635	605	463	440	701	671	396	384

Table A.28: Shear rate data (s^{-1}) obtained for the chocolate samples at 40°C using the Carri-Med rheometer and coaxial cylinder fixture 5222 for controlled stress tests at ascending (asc) and descending (dsc) shear stress.

Shear Stress	HMC		HSS		H1		H2	
(Pa)	asc	dsc	asc	dsc	asc	dsc	asc	dsc
1.926							0.0097	
3.852		0.0370		0.0292		0.0341	0.0585	0.0390
5.778		0.0409						
7.704	0.0409	0.0672					0.0624	
9.630	0.0502	0.0916		0.0546		0.0609	0.0526	0.0646
11.55	0.0653	0.1098	0.0464	0.0624	0.0276		0.0438	
13.48	0.0887	0.1287	0.0487	0.0766	0.0448	0.0819	0.0465	0.0890
15.40	0.0887	0.1506	0.0660	0.0838	0.0600	0.1033	0.0746	0.1105
17.33	0.1124	0.1669	0.0858	0.0950	0.0721	0.1009	2.133	0.1293
19.26	0.1331	0.1862	0.0782	0.1121	0.0835	0.1186	0.0975	0.1456
21.18	0.1566	0.2089	0.0939	0.1272	0.0945	0.1394	0.1075	0.1589
23.11	0.1725	0.2386	0.1062	0.1423	0.1092	0.1599	0.1219	0.1618
25.03	0.1955	0.2652	0.1184	0.1587	0.1221	0.1742	0.1431	0.1963
26.96	0.2150	0.2983	2.571	0.1811	0.1433	0.1907	0.1584	0.2154
28.89	0.2396	0.3332	0.1494	0.2006	0.1550	0.2083	0.1840	0.2392
30.81	0.2615	0.3741	0.1689	0.2259	0.1807	0.2307	0.1984	0.2678
32.74	0.2896	0.4214	0.1930	0.2596	0.1943	0.2528	0.2203	0.2925
34.66	0.3190	0.4748	0.2157	0.2991	0.2122	0.2756	0.2369	0.3233
36.59	0.3502	0.5228	0.2362	0.3451	0.2307	0.2986	0.2554	0.3490
38.52	0.3802	0.5796	0.2691	0.4027	0.2509	0.3185	0.2854	0.3809
40.44	0.4158	0.6593	0.3005	0.4655	0.2739	0.3522	0.3125	0.4225
42.37	0.4592	0.7322	0.3337	0.5423	0.2951	0.3744	0.3383	0.4608
44.29	0.5040	0.8163	0.3771	0.6283	0.3120	0.3987	0.3622	0.5076
46.22	0.5577	0.9003	0.4297	0.7317	0.3377	0.4211	0.3919	0.5557
48.15	0.6162	0.9894	0.4858	0.8462	0.3584	0.4536	0.4239	0.6097
50.07	0.6766	1.081	0.5503	0.9554	0.3805	0.4846	0.4526	0.6659
52.00	0.7539	1.181	0.6242	1.089	0.3698	0.5158	0.4797	0.7215
53.92	0.8187	1.288	0.7021	1.217	0.4316	0.5430	0.5228	0.8044
55.85	0.8945	1.379	0.7852	1.346	0.4579	0.5772	0.5574	0.8631
57.78	0.9983	1.498	0.8967	1.516	0.4914	0.6070	0.6118	0.9262
59.70	1.044	1.620	1.004	1.677	0.5196	0.5599	0.6600	1.021
61.63	1.183	1.723	1.116	1.825	0.5447	0.6769	0.7056	1.091
63.55	1.279	1.835	1.248	1.998	0.5749	0.7253	0.7595	1.173
65.48	1.385	1.916	1.377	2.166	0.5970	0.7588	0.8192	1.252
67.41	1.484	2.059	1.524	2.336	0.6230	0.7975	0.8865	1.347

continued...

Table A.28 continued.

Shear Stress (Pa)	HMC		HSS		H1		H2	
	asc	dsc	asc	dsc	asc	dsc	asc	dsc
69.33	1.590	2.193	1.659	2.497	0.6649	0.8460	0.9587	1.450
71.26	1.694	2.303	1.820	2.684	0.4686	0.9025	1.038	1.539
73.18	1.795	2.426	1.975	2.875	0.3714	0.9476	1.110	1.631
75.11	1.918	2.562	2.129	3.041	0.7608	0.9971	1.203	1.731
77.04	2.030	2.682	2.293	3.262	0.8229	1.057	1.276	1.829
78.96	2.126	2.612	2.443	3.424	0.8609	1.006	1.373	1.937
80.89	2.224	2.909	2.597	3.600	0.8943	0.9177	1.465	2.023
82.81	2.339	3.031	2.778	3.825	0.9386	1.223	1.543	1.463
84.74	2.475	3.165	2.948	3.997	0.9984	1.286	1.633	2.244
86.67	2.576	3.297	3.085	4.202	1.046	1.358	1.741	2.078
88.59	2.677	3.409	3.228	4.398	1.092	1.426	1.838	1.894
90.52	2.795	3.507	3.378	4.588	1.143	1.495	1.926	1.873
92.44	2.887	3.638	3.515	4.786	1.206	1.579	2.026	2.858
94.37	3.004	3.763	3.669	4.983	1.256	1.634	2.135	2.976
96.30	3.103	3.902	3.819	5.225	1.325	1.357	2.236	3.111
98.22	3.208	4.022	3.987	5.410	1.354	1.808	2.339	3.228
100.1	3.311	4.141	4.176	5.634	1.454	1.880	2.455	3.350
102.0	3.418	4.285	4.328	5.851	1.530	1.968	2.554	3.503
104.0	3.531	4.412	4.514	6.061	1.589	2.047	2.647	3.593
105.9	3.601	4.512	4.677	6.273	1.651	1.775	2.758	3.727
107.8	3.764	4.640	4.840	6.481	1.732	2.221	2.868	3.875
109.7	3.873	4.785	5.027	6.681	1.827	2.370	2.981	4.004
111.7	4.003	4.926	5.201	6.921	1.901	2.411	3.063	4.123
113.6	4.067	5.029	5.373	7.112	1.976	2.490	3.193	4.265
115.5	4.222	4.965	5.563	7.354	2.081	2.574	3.310	4.389
117.4	4.336	5.281	5.735	7.586	2.153	2.670	3.400	4.463
119.4	4.459	5.434	5.917	7.796	2.245	2.761	3.532	4.633
121.3	4.576	5.549	6.101	8.017	2.337	2.835	3.662	4.808
123.2	4.697	5.691	6.273	8.218	2.417	2.957	3.778	4.922
125.1	4.837	5.848	6.475	8.450	2.478	3.051	3.912	5.079
127.1	4.945	5.945	6.649	8.660	2.587	3.146	4.023	5.198
129.0	5.074	6.074	6.853	8.924	2.686	3.243	4.139	5.297
130.9	5.196	6.215	7.021	9.124	2.766	3.352	4.292	5.457
132.8	5.292	6.333	7.270	9.393	2.751	3.449	4.393	5.579
134.8	5.440	6.483	7.449	9.603	2.969	3.030	4.529	5.742
136.7	5.527	6.595	7.625	9.800	3.066	3.662	4.649	5.872
138.6	5.675	6.710	7.829	10.02	3.135	3.807	4.751	5.989

continued...

Table A.28 continued.

Shear Stress (Pa)	HMC		HSS		H1		H2	
	asc	dsc	asc	dsc	asc	dsc	asc	dsc
140.5	5.820	6.865	8.049	10.27	3.255	3.870	4.903	6.002
142.5	5.925	7.013	8.230	10.47	3.357	3.965	5.052	6.300
144.4	6.041	6.573	8.401	10.69	3.415	4.045	5.158	6.439
146.3	6.197	7.266	8.657	10.98	3.533	4.183	5.299	6.591
148.3	6.292	7.413	8.850	11.21	3.634	4.263	5.448	6.726
150.2	6.401	7.535	9.063	11.43	3.700	4.420	5.572	6.866
152.1	6.533	7.652	9.245	11.67	3.788	4.500	5.689	7.008
154.0	6.632	7.672	9.434	11.91	3.807	4.574	5.827	7.098
156.0	6.749	7.916	9.626	12.13	3.968	4.690	5.943	6.986
157.9	6.800	7.997	9.795	12.26	4.059	4.371	6.045	7.354
159.8	6.966	8.174	10.09	12.58	4.203	4.913	6.191	7.543
161.7	7.106	8.327	10.36	12.90	4.291	4.962	6.303	7.639
163.7	7.226	8.356	10.50	13.04	4.435	5.111	6.431	7.819
165.6	7.376	8.607	10.78	13.31	4.603	4.218	6.562	7.966
167.5	7.456	8.077	10.92	13.50	3.912	5.346	6.705	8.120
169.4	7.600	8.872	11.22	13.80	4.916	5.454	6.848	7.457
171.4	7.692	8.948	11.36	14.02	5.000	5.578	6.527	8.420
173.3	7.862	9.151	11.63	14.31	5.157	5.718	7.100	8.604
175.2	7.930	9.226	11.75	14.46	5.242	5.793	7.216	8.693
177.1	8.013	9.346	11.90	14.57	5.302	5.810	7.294	8.784
179.1	8.172	9.531	12.18	14.95	5.459	6.012	7.445	8.951
181.0	8.284	9.601	12.30	15.10	5.518	6.134	7.554	8.362
182.9	8.467	9.779	12.64	15.44	5.626	6.252	7.721	9.305
184.8	8.535	9.916	12.81	15.57	5.115	6.306	7.782	9.467
186.8	8.610	9.949	13.10	15.90	5.801	6.409	7.890	8.616
188.7	8.816	10.16	13.29	16.09	5.944	6.041	8.066	9.698
190.6	8.989	10.34	13.60	16.47	6.089	6.096	8.249	9.867
192.6	9.094	10.47	13.76	16.60	6.123	6.852	8.364	8.918
194.5	9.176	10.56	13.91	16.76	5.715	6.881	8.440	9.034
196.4	9.369	10.77	14.19	17.16	6.325	6.794	8.388	9.227
198.3	9.443	10.83	14.44	17.31	6.407	7.156	8.753	9.310
200.3	9.543	11.00	14.62	17.50	6.320	7.169	8.847	9.385
202.2	9.745	11.14	14.95	17.84	6.633	7.417	9.026	8.572
204.1	9.851	11.26	15.13	18.00	6.715	7.505	9.126	9.719
206.0	9.955	11.38	15.27	18.19	5.674	7.575	9.232	9.774
208.0	10.15	11.52	15.63	18.55	6.928	7.014	9.413	10.02
209.9	10.25	11.46	15.83	18.77	6.995	7.841	9.572	10.12

continued...

Table A.28 continued.

Shear Stress (Pa)	HMC		HSS		H1		H2	
	asc	dsc	asc	dsc	asc	dsc	asc	dsc
211.8	10.35	11.76	16.08	19.03	7.083	6.842	9.637	10.18
213.7	10.54	11.94	16.36	19.27	7.153	8.051	9.760	10.28
215.7	10.62	12.05	16.55	19.48	7.355	8.213	9.945	10.52
217.6	10.78	12.19	16.64	19.68	7.406	8.251	10.06	10.64
219.5	10.92	12.42	17.06	20.02	7.574	8.467	10.27	9.989
221.4	11.07	12.49	17.22	20.22	7.685	8.490	10.42	10.96
223.4	11.17	12.64	17.47	20.40	7.775	8.706	10.48	11.03
225.3	11.29	12.78	17.81	20.77	7.973	8.864	10.73	11.26
227.2	11.47	12.86	18.02	20.98	8.065	8.940	10.84	11.30
229.1	11.61	13.01	18.21	21.16	8.156	9.029	10.96	11.44
231.1	11.63	13.13	18.43	21.36	8.284	7.130	11.05	11.55
233.0	11.83	12.44	18.63	21.53	8.303	9.279	11.16	11.69
234.9	11.99	13.45	18.97	21.93	8.618	9.374	11.44	11.86
236.8	11.96	13.54	19.18	22.10	8.669	9.506	11.52	11.93
238.8	12.34	13.78	19.59	22.49	8.750	9.582	11.65	11.97
240.7	12.42	13.87	19.82	22.71	8.929	9.854	11.79	12.28
242.6	11.92	13.96	20.01	22.86	9.076	9.912	11.95	12.41
244.6	12.72	14.12	20.21	23.12	9.208	10.02	12.12	12.52
246.5	12.77	14.09	20.42	23.27	9.309	10.10	12.17	12.67
248.4	12.96	14.41	20.83	23.70	9.442	9.463	12.45	12.92
250.3	13.12	14.56	21.06	23.90	9.582	10.44	12.55	13.00
252.3	13.37	14.54	21.27	24.05	9.708	10.52	12.29	13.08
254.2	13.34	14.75	21.43	24.30	9.768	10.65	12.82	13.25
256.1	13.46	14.85	21.71	24.48	9.853	10.73	12.94	11.86
258.0	13.66	15.16	22.10	24.91	10.06	10.94	13.16	13.58
260.0	13.81	15.24	22.33	25.08	10.20	11.05	13.26	13.67
261.9	13.87	15.32	22.56	25.28	10.28	9.364	13.42	13.66
263.8	14.08	15.49	22.77	25.49	10.38	11.22	13.52	13.84
265.7	14.29	15.54	23.22	25.89	10.59	11.41	13.72	14.08
267.7	14.15	15.54	23.43	26.11	10.73	11.36	13.86	13.86
269.6	14.56	15.91	23.66	26.32	10.81	11.73	14.05	14.33
271.5	14.64	16.00	23.90	26.52	10.68	11.82	14.15	14.48
273.4	14.77	16.15	24.15	26.74	10.97	11.90	14.37	14.59
275.4	14.78	16.26	24.35	26.92	11.20	11.78	14.40	14.67
277.3	14.94	16.38	24.61	27.15	11.28	12.13	14.62	14.85
279.2	15.23	16.46	25.03	27.57	11.47	10.62	14.83	15.05
281.1	15.12	16.72	25.26	27.76	11.60	12.40	14.89	15.19

continued...

Table A.28 continued.

Shear Stress (Pa)	HMC		HSS		H1		H2	
	asc	dsc	asc	dsc	asc	dsc	asc	dsc
283.1	15.52	16.84	25.53	28.00	11.62	12.57	15.06	15.32
285.0	15.60	16.99	25.68	28.19	11.80	12.71	15.18	15.44
286.9	15.77	17.05	26.02	28.40	11.99	12.78	15.30	15.51
288.9	16.04	17.33	26.42	28.86	12.00	12.93	15.48	15.72
290.8	15.80	17.45	26.65	29.04	12.06	11.28	15.69	15.86
292.7	16.29	17.57	26.90	29.24	11.59	13.25	15.86	15.99
294.6	16.37	17.70	27.07	29.45	12.50	13.34	16.04	16.08
296.6	16.56	17.79	27.38	29.66	12.61	13.40	16.23	16.28
298.5	16.69	17.93	27.62	29.91	12.74	13.62	16.11	16.36
300.4	16.80	18.02	27.80	30.16	12.85	13.59	16.47	16.52
302.3	16.23	18.14	28.08	30.32	12.93	13.44	16.59	16.57
304.3	16.89	18.23	28.36	30.49	13.10	13.93	16.72	16.69
306.2	17.20	18.40	28.58	30.72	13.21	14.00	16.93	16.83
308.1	16.87	18.35	28.82	31.00	11.56	14.21	17.07	16.92
310.0	17.46	18.63	29.04	31.17	13.39	14.30	17.16	17.08
312.0	17.65	18.75	29.47	31.61	13.62	14.53	17.41	17.26
313.9	17.93	19.04	29.81	31.84	11.95	14.68	17.56	17.37
315.8	18.03	18.94	30.04	32.06	13.94	14.73	17.71	17.43
317.7	18.16	19.28	30.31	32.26	14.06	14.91	17.93	17.69
319.7	18.31	19.33	30.47	32.41	14.17	15.00	19.24	17.78
321.6	18.44	19.49	30.77	32.64	14.28	15.06	18.21	17.94
323.5	18.70	19.71	31.29	33.10	14.46	15.13	18.36	18.09
325.4	18.90	19.88	31.56	33.37	14.60	15.39	18.54	18.14
327.4	19.00	20.02	31.80	33.59	14.77	15.61	18.80	18.43
329.3	19.13	20.14	32.03	33.74	15.01	15.67	18.90	18.48
331.2	19.20	20.23	32.16	33.93	15.13	15.80	19.01	17.34
333.1	19.37	20.38	32.50	34.17	15.21	15.91	19.21	18.75
335.1	19.25	20.49	32.86	34.35	15.39	16.05	19.43	18.91
337.0	19.76	18.53	33.19	34.63	15.43	16.19	18.86	19.00
338.9	19.90	21.88	33.43	34.88	15.62	16.36	19.78	19.19
340.9	20.01	20.62	33.62	35.11	15.79	16.35	19.92	19.30
342.8	20.04	21.00	33.81	35.28	15.89	16.60	20.15	19.43
344.7	20.33	20.64	34.05	35.44	16.15	16.62	20.22	19.46
346.6	19.94	21.29	34.44	35.64	16.13	16.71	19.64	19.08
348.6	20.68	21.37	34.67	35.95	16.27	16.92	20.57	19.61
350.5	20.33	21.45	35.00	36.17	15.48	16.97	20.73	19.81
352.4	20.92	21.56	35.21	36.38	16.58	17.21	20.87	19.97

continued...

Table A.28 continued.

Shear Stress (Pa)	HMC		HSS		H1		H2	
	asc	dsc	asc	dsc	asc	dsc	asc	dsc
354.3	21.21	21.74	35.65	36.79	16.74	16.34	21.14	20.09
356.3	21.39	21.96	35.93	36.94	16.94	17.38	21.30	20.30
358.2	21.54	21.58	36.24	37.15	17.14	17.71	21.58	20.41
360.1	21.70	22.25	36.57	37.37	17.37	17.82	21.70	20.50
362.0	21.85	22.31	36.84	37.60	17.24	17.83	21.88	20.69
364.0	21.75	22.44	37.15	37.81	17.51	17.94	22.07	20.84
365.9	21.49	22.59	37.48	38.04	17.69	18.03	22.19	20.94
367.8	22.26	22.20	37.67	38.27	17.97	18.22	22.41	21.07
369.7	22.51	22.85	38.00	38.52	18.02	16.28	22.56	21.20
371.7	22.64	22.94	38.27	38.70	18.20	18.47	22.71	21.34
373.6	22.47	23.08	38.51	38.85	18.28	18.48	22.88	21.40
375.5	22.98	23.18	38.74	39.04	16.67	18.69	23.02	21.57
377.4	23.08	23.00	38.99	39.25	18.64	18.71	23.24	21.64
379.4	23.29	23.47	39.22	39.53	18.80	18.88	23.46	21.71
381.3	23.40	23.59	39.58	39.70	18.98	19.10	23.61	21.85
383.2	23.61	23.58	39.84	39.90	19.11	19.24	23.78	21.90
385.2	23.77	23.81	40.07	40.12	19.28	19.25	24.00	22.13

Table A.29: Shear rate data (s^{-1}) for chocolate sample H1 at 40°C obtained with the Carri-Med rheometer and coaxial cylinder fixture 5222 for controlled stress tests at ascending (asc) and descending (dsc) shear stress for 12 and 30 minute run times.

12 min run			30 min run		
Shear Stress (Pa)	Shear rate (s^{-1}) asc	dsc	Shear Stress (Pa)	Shear rate (s^{-1}) asc	dsc
12.11		0.0673	5.813		0.0166
14.53		0.0683	8.720		0.0322
16.95		0.0904	10.17	0.0161	0.0335
19.38		0.1096	11.63	0.0312	0.0452
21.80	0.0507	0.1259	13.08	0.0307	0.0537
24.22	0.0493	0.1513	14.53	0.0290	0.0641
26.64	0.0644	0.1740	15.98	0.0468	0.0777
29.06	0.1034	0.1997	17.44	0.0426	0.0917
31.48	0.0937	0.2267	18.89	0.0514	0.1057
33.91	0.1165	0.2531	20.34	0.0615	0.1204
36.33	0.1412	0.2804	21.80	0.0748	0.1353
38.75	0.1601	0.3149	23.25	0.0862	0.1493
41.17	0.1805	0.3458	24.70	0.0992	0.1646
43.59	0.2046	0.3757	26.16	0.1106	0.1783
46.02	0.2261	0.4089	27.61	0.1220	0.1939
48.44	0.2472	0.4473	29.06	0.1350	0.2082
50.86	0.2742	0.4840	30.52	0.1513	0.2277
53.28	0.3009	0.5218	31.97	0.1653	0.2375
55.70	0.3243	0.5628	33.42	0.1802	0.2521
58.13	0.3523	0.6008	34.88	0.1958	0.2658
60.55	0.3822	0.6434	36.33	0.2111	0.2807
62.97	0.4147	0.6897	37.78	0.2297	0.2941
65.39	0.4473	0.7326	39.24	0.2437	0.3087
67.81	0.4798	0.7837	40.69	0.2583	0.3240
70.24	0.5065	0.8373	42.14	0.2723	0.3370
72.66	0.5367	0.8881	43.59	0.2853	0.3520
75.08	0.5696	0.9496	45.05	0.2986	0.3679
77.50	0.6005	1.011	46.50	0.3155	0.3832
79.92	0.6386	1.073	47.95	0.3295	0.3972
82.35	0.6698	1.145	49.41	0.3412	0.4229
84.77	0.7040	1.218	50.86	0.3556	0.4392

continued...

Table A.29 continued.

12 min run			30 min run		
Shear Stress (Pa)	Shear rate (s^{-1}) asc	dsc	Shear Stress (Pa)	Shear rate (s^{-1}) asc	dsc
87.19	0.7446	1.299	52.31	0.3725	0.4613
89.61	0.7879	1.384	53.77	0.3865	0.4779
92.03	0.8393	1.464	55.22	0.4017	0.4951
94.45	0.8917	1.565	56.67	0.4203	0.5127
96.88	0.9362	1.651	58.13	0.4352	0.5306
99.30	0.9935	1.748	59.58	0.4512	0.5442
101.7	1.048	1.841	61.03	0.4678	0.5673
104.1	1.113	1.947	62.49	0.4821	0.5829
106.6	1.177	2.049	63.94	0.5000	0.5992
109.0	1.251	2.157	65.39	0.5156	0.6155
111.4	1.335	2.257	66.84	0.5293	0.6421
113.8	1.414	2.374	68.30	0.5426	0.6581
116.3	1.490	2.491	69.75	0.5592	0.6861
118.7	1.592	2.602	71.20	0.5794	0.7241
121.1	1.693	2.724	72.66	0.6002	0.7687
123.5	1.794	2.842	74.11	0.6187	0.7999
125.9	1.907	2.961	75.56	0.6392	0.8354
128.4	2.020	3.086	77.02	0.6578	0.8744
130.8	2.129	3.221	78.47	0.6795	0.9089
133.2	2.254	3.344	79.92	0.7036	0.9447
135.6	2.383	3.465	81.38	0.7225	0.9824
138.0	2.501	3.599	82.83	0.7443	1.016
140.5	2.612	3.719	84.28	0.7703	1.058
142.9	2.739	3.872	85.74	0.7970	1.096
145.3	2.865	4.003	87.19	0.8243	1.139
147.7	3.009	4.132	88.64	0.8487	1.181
150.2	3.155	4.270	90.10	0.8777	1.225
152.6	3.285	4.400	91.55	0.9027	1.270
155.0	3.407	4.527	93.00	0.9323	1.316
157.4	3.550	4.665	94.45	0.9635	1.365
159.8	3.681	4.809	95.91	0.9941	1.419
162.3	3.807	5.027	97.36	1.032	1.469
164.7	3.937	5.104	98.81	1.068	1.520
167.1	4.068	5.268	100.3	1.107	1.576

continued...

Table A.29 continued.

12 min run			30 min run		
Shear Stress (Pa)	Shear rate (s^{-1}) asc	dsc	Shear Stress (Pa)	Shear rate (s^{-1}) asc	dsc
169.5	4.223	5.390	101.7	1.144	1.623
172.0	4.362	5.517	103.2	1.189	1.673
174.4	4.478	5.684	104.6	1.240	1.723
176.8	4.584	5.806	106.1	1.282	1.782
179.2	4.726	5.970	107.5	1.322	1.838
181.6	4.869	6.141	109.0	1.374	1.903
184.1	5.059	6.278	110.4	1.423	1.956
186.5	5.297	6.384	111.9	1.478	2.021
188.9	5.539	6.560	113.3	1.524	2.084
191.3	5.638	6.730	114.8	1.597	2.149
193.8	5.683	6.836	116.3	1.659	2.213
196.2	5.727	7.029	117.7	1.721	2.276
198.6	5.819	7.193	119.2	1.779	2.340
201.0	5.992	7.335	120.6	1.834	2.407
203.4	6.123	7.476	122.1	1.897	2.471
205.9	6.223	7.629	123.5	1.959	2.540
208.3	6.304	7.758	125.0	2.022	2.595
210.7	6.408	7.948	126.4	2.086	2.663
213.1	6.533	8.100	127.9	2.139	2.732
215.6	6.698	8.249	129.3	2.202	2.793
218.0	6.804	8.386	130.8	2.269	2.871
220.4	6.947	8.596	132.2	2.343	2.929
222.8	7.068	8.724	133.7	2.415	3.002
225.2	7.255	8.888	135.1	2.469	3.067
227.7	7.397	9.089	136.6	2.536	3.139
230.1	7.558	9.172	138.0	2.595	3.205
232.5	7.698	9.340	139.5	2.654	3.269
234.9	7.785	9.483	141.0	2.702	3.339
237.3	7.962	9.663	142.4	2.753	3.402
239.8	8.114	9.810	143.9	2.816	3.475
242.2	8.244	10.00	145.3	2.892	3.535
244.6	8.348	10.16	146.8	2.961	3.623
247.0	8.530	10.29	148.2	3.028	3.674
249.5	8.685	10.42	149.7	3.093	3.766

continued...

Table A.29 continued.

12 min run			30 min run		
Shear Stress (Pa)	Shear rate (s^{-1}) asc	dsc	Shear Stress (Pa)	Shear rate (s^{-1}) asc	dsc
251.9	8.761	10.62	151.1	3.127	3.828
254.3	8.918	10.82	152.6	3.184	3.881
256.7	9.126	10.97	154.0	3.258	3.960
259.1	9.266	11.14	155.5	3.329	4.024
261.6	9.385	11.29	156.9	3.424	4.088
264.0	9.543	11.44	158.4	3.468	4.144
266.4	9.635	11.66	159.8	3.529	4.210
268.8	9.800	11.77	161.3	3.603	4.271
271.3	9.942	11.99	162.8	3.664	4.382
273.7	10.04	12.16	164.2	3.726	4.440
276.1	10.27	12.30	165.7	3.819	4.522
278.5	10.42	12.46	167.1	3.884	4.595
280.9	10.55	12.66	168.6	3.947	4.651
283.4	10.74	12.81	170.0	4.007	4.715
285.8	10.86	13.00	171.5	4.050	4.798
288.2	11.03	13.16	172.9	4.103	4.892
290.6	11.23	13.36	174.4	4.164	4.973
293.1	11.39	13.47	175.8	4.251	5.041
295.5	11.55	13.67	177.3	4.344	5.080
297.9	11.67	13.83	178.7	4.412	5.164
300.3	11.87	13.98	180.2	4.455	5.236
302.7	12.02	14.20	181.6	4.533	5.298
305.2	12.18	14.37	183.1	4.601	5.364
307.6	12.35	14.45	184.6	4.685	5.434
310.0	12.52	14.65	186.0	4.742	5.492
312.4	12.69	14.86	187.5	4.805	5.570
314.8	12.80	14.95	188.9	4.865	5.624
317.3	13.03	15.20	190.4	4.937	5.726
319.7	13.16	15.38	191.8	4.999	5.819
322.1	13.29	15.52	193.3	5.076	5.837
324.5	13.52	15.74	194.7	5.173	5.908
327.0	13.60	15.85	196.2	5.186	6.031
329.4	13.72	16.07	197.6	5.253	6.121
331.8	13.85	16.20	199.1	5.365	6.116

continued...

Table A.29 continued.

12 min run			30 min run		
Shear Stress (Pa)	Shear rate (s^{-1}) asc	dsc	Shear Stress (Pa)	Shear rate (s^{-1}) asc	dsc
334.2	14.15	16.38	200.5	5.466	6.254
336.6	14.26	16.63	202.0	5.458	6.312
339.1	14.37	16.75	203.4	5.581	6.422
341.5	14.72	16.93	204.9	5.661	6.428
343.9	14.76	17.07	206.3	5.756	6.531
346.3	15.01	17.24	207.8	5.770	6.615
348.8	15.21	17.35	209.3	5.905	6.652
351.2	15.36	17.54	210.7	6.002	6.738
353.6	15.57	17.81	212.2	6.033	6.844
356.0	15.82	17.89	213.6	6.138	6.825
358.4	16.03	18.13	215.1	6.250	6.972
360.9	16.73	18.26	216.5	6.240	7.085
363.3	16.35	18.41	218.0	6.346	7.072
365.7	16.61	18.63	219.4	6.461	7.197
368.1	16.78	18.73	220.9	6.438	7.284
370.6	17.02	18.87	222.3	6.572	7.301
373.0	17.18	18.98	223.8	6.663	7.409
375.4	17.38	19.21	225.2	6.690	7.501
377.8	17.52	19.33	226.7	6.814	7.541
380.2	17.76	19.52	228.1	6.930	7.635
382.7	17.96	19.62	229.6	6.965	7.673
385.1	18.09	19.80	231.1	7.092	7.755
387.5	18.39	19.99	232.5	7.148	7.838
389.9	18.49	20.06	234.0	7.246	7.925
392.4	18.73	20.38	235.4	7.324	8.013
394.8	18.96	20.40	236.9	7.433	8.089
397.2	19.22	20.61	238.3	7.507	8.189
399.6	19.34	20.89	239.8	7.589	8.264
402.0	19.55	21.06	241.2	7.657	8.355
404.5	19.82	21.22	242.7	7.736	8.428
406.9	19.95	21.55	244.1	7.836	8.472
409.3	20.21	21.66	245.6	7.926	8.591
411.7	20.42	21.89	247.0	8.011	8.601
414.1	20.62	21.90	248.5	8.125	8.722

continued...

Table A.29 continued.

12 min run			30 min run		
Shear Stress (Pa)	Shear rate (s^{-1}) asc	dsc	Shear Stress (Pa)	Shear rate (s^{-1}) asc	dsc
416.6	20.78	22.16	249.9	8.163	8.758
419.0	20.89	22.19	251.4	8.317	8.839
421.4	21.21	22.30	252.8	5.561	8.908
423.8	21.33	22.25	254.3	8.452	9.030
426.3	21.45	22.39	255.8	8.540	9.117
428.7	21.65	22.58	257.2	8.653	9.195
431.1	21.83	22.95	258.7	8.761	9.304
433.5	22.01	23.21	260.1	8.834	9.375
435.9	22.12	23.24	261.6	8.921	9.380
438.4	22.33	23.41	263.0	9.010	9.503
440.8	22.54	23.64	264.5	9.023	9.507
443.2	22.71	23.80	265.9	9.170	9.649
445.6	22.92	23.83	267.4	9.205	9.704
448.1	23.07	23.85	268.8	9.348	9.819
450.5	23.15	23.92	270.3	9.437	9.909
452.9	23.21	24.05	271.7	9.540	9.979
455.3	23.49	24.27	273.2	9.663	10.08
457.7	23.62	24.39	274.6	9.787	10.18
460.2	23.86	24.45	276.1	9.881	10.26
462.6	24.05	24.74	277.6	9.981	10.25
465.0	24.01	24.90	279.0	10.07	10.34
467.4	24.36	24.88	280.5	10.12	10.42
469.9	24.36	25.11	281.9	10.20	10.52
472.3	24.76	25.61	283.4	10.29	10.62
474.7	24.80	25.62	284.8	10.40	10.70
477.1	25.12	25.59	286.3	10.54	10.79
479.5	25.30	25.53	287.7	10.66	10.81
482.0	25.56	25.76	289.2	10.73	10.89
484.4	25.87	25.89	290.6	10.76	10.89

Table A.30: Shear rate data (s^{-1}) for chocolate sample H2 at 40°C obtained with the Carri-Med rheometer and coaxial cylinder fixture 5222 for controlled stress tests at ascending (asc) and descending (dsc) shear stress for 12 and 30 minute run times.

12 min run			30 min run		
Shear Stress (Pa)	Shear rate (s^{-1}) asc	dsc	Shear Stress (Pa)	Shear rate (s^{-1}) asc	dsc
2.880		0.0196	2.880		0.0255
3.840		0.0235	4.320		0.2650
5.760		0.0304	5.760		0.0338
6.720	0.0647		7.200	0.0147	0.0399
7.680		0.0368	8.640	0.0294	0.0477
8.640	0.0376	0.0441	10.08	0.0284	0.0529
9.600		0.0405	11.52	0.0412	0.0611
10.56	0.0524	0.0549	12.96	0.0490	0.0722
11.52	0.0510	0.0598	14.40	0.0598	0.0885
12.48	0.0583	0.0666	15.84	0.0679	0.1153
13.44	0.0666	0.0745	17.28	0.0846	0.1669
14.40	0.0728	0.0848	18.72	0.1049	0.2434
15.36	0.0853	0.1019	20.16	0.1287	0.3489
16.32	0.1034	0.1241	21.60	0.1650	0.4711
17.28	0.1169	0.1509	23.04	0.2163	0.6233
18.24	0.1294	0.1797	24.48	0.2822	0.7863
19.20	0.1548	0.2296	25.92	0.3747	0.9692
20.16	0.1839	0.2858	27.36	0.4893	1.156
21.12	0.2127	0.3593	28.80	0.6324	1.348
22.08	0.2502	0.4384	30.24	0.7928	1.554
23.04	0.2960	0.5250	31.68	0.9607	1.768
24.00	0.3479	0.6256	33.12	1.141	1.981
24.96	0.4096	0.7249	34.56	1.324	2.205
25.92	0.4880	0.8314	36.00	1.513	2.440
26.88	0.5713	0.9447	37.44	1.705	2.647
27.84	0.6657	1.061	38.88	1.904	2.907
28.80	0.7742	1.174	40.32	2.088	3.162
29.76	0.9104	1.302	41.76	2.305	3.383
30.72	1.003	1.431	43.20	2.532	3.663
31.68	1.133	1.561	44.64	2.718	3.919
32.64	1.265	1.695	46.08	2.952	4.146

continued...

Table A.30 continued.

12 min run			30 min run		
Shear Stress (Pa)	Shear rate (s^{-1}) asc	dsc	Shear Stress (Pa)	Shear rate (s^{-1}) asc	dsc
33.60	1.403	1.831	47.52	3.176	4.392
34.56	1.551	1.969	48.96	3.379	4.692
35.52	1.691	2.103	50.40	3.585	4.923
36.48	1.820	2.254	51.84	3.836	5.204
37.44	1.946	2.382	53.28	4.047	5.478
38.40	2.073	2.534	54.72	4.294	5.762
39.36	2.197	2.695	56.16	4.524	6.003
40.32	2.331	2.843	57.60	4.763	6.285
41.28	2.472	3.011	59.04	4.992	6.588
42.24	2.625	3.144	60.48	5.223	6.836
43.20	2.786	3.302	61.92	5.490	7.095
44.16	2.912	3.458	63.36	5.705	7.400
45.12	3.067	3.623	64.80	5.934	7.727
46.08	3.227	3.768	66.24	6.230	7.989
47.04	3.386	3.933	67.68	6.483	8.289
48.00	3.523	4.086	69.12	6.726	8.537
48.96	3.659	4.249	70.56	6.980	8.859
49.92	3.790	4.436	72.00	7.228	9.149
50.88	3.922	4.571	73.44	7.492	9.422
51.84	4.079	4.726	74.88	7.736	9.705
52.80	4.199	4.911	76.32	8.010	9.996
53.76	4.333	5.079	77.76	8.245	10.31
54.72	4.511	5.237	79.20	8.518	10.57
55.68	4.676	5.426	80.64	8.780	10.87
56.64	4.817	5.587	82.08	9.018	11.13
57.60	5.010	5.776	83.52	9.275	11.42
58.56	5.160	5.927	84.96	9.559	11.73
59.52	5.349	6.085	86.40	9.795	12.00
60.48	5.503	6.291	87.84	10.05	12.34
61.44	5.654	6.458	89.28	10.31	12.63
62.40	5.848	6.611	90.72	10.63	12.93
63.36	5.990	6.819	92.16	10.88	13.21
64.32	6.118	6.963	93.60	11.16	13.52
65.28	6.306	7.153	95.04	11.40	13.83

continued...

Table A.30 continued.

12 min run			30 min run		
Shear Stress (Pa)	Shear rate (s^{-1}) asc	dsc	Shear Stress (Pa)	Shear rate (s^{-1}) asc	dsc
66.24	6.425	7.325	96.48	11.69	14.13
67.20	6.594	7.511	97.92	11.97	14.40
68.16	6.764	7.684	99.36	12.26	14.73
69.12	6.943	7.875	100.8	12.52	15.02
70.08	7.110	8.016	102.2	12.80	15.26
71.04	7.277	8.211	103.7	13.05	15.61
72.00	7.408	8.393	105.1	13.29	15.89
72.96	7.550	8.559	106.6	13.60	16.21
73.92	7.719	8.743	108.0	13.86	16.55
74.88	7.912	8.934	109.4	14.15	16.81
75.84	8.075	9.111	110.9	14.46	17.14
76.80	8.253	9.331	112.3	14.71	17.42
77.76	8.402	9.454	113.8	15.03	17.76
78.72	8.597	9.637	115.2	15.31	18.05
79.68	8.745	9.807	116.6	15.59	18.33
80.64	8.924	9.981	118.1	15.88	18.66
81.60	9.057	10.20	119.5	16.15	18.98
82.56	9.236	10.36	121.0	16.46	19.30
83.52	9.424	10.52	122.4	16.72	19.59
84.48	9.616	10.73	123.8	17.02	19.86
85.44	9.758	10.89	125.3	17.35	20.18
86.40	9.931	11.07	126.7	17.64	20.55
87.36	10.11	11.27	128.2	17.87	20.78
88.32	10.28	11.47	129.6	18.19	21.13
89.28	10.44	11.64	131.0	18.46	21.42
90.24	10.65	11.83	132.5	18.79	21.76
91.20	10.84	11.97	133.9	19.05	22.03
92.16	11.00	12.16	135.4	19.39	22.37
93.12	11.15	12.36	136.8	19.64	22.66
94.08	11.35	12.56	138.2	19.95	22.98
95.04	11.52	12.69	139.7	20.25	23.24
96.00	11.71	12.93	141.1	20.55	23.64
96.96	11.86	13.09	142.6	20.81	23.86
97.92	12.05	13.27	144.0	21.14	24.16
98.88	12.25	13.49	145.4	21.41	24.52

continued...

Table A.30 continued.

12 min run			30 min run		
Shear Stress (Pa)	Shear rate (s^{-1}) asc	dsc	Shear Stress (Pa)	Shear rate (s^{-1}) asc	dsc
99.84	12.40	13.63	146.9	21.69	24.81
100.8	12.58	13.85	148.3	22.05	25.16
101.8	12.79	14.04	149.8	22.31	25.42
102.7	12.95	14.19	151.2	22.65	25.73
103.7	13.16	14.43	152.6	22.94	26.06
104.6	13.29	14.58	154.1	23.20	26.33
105.6	13.55	14.77	155.5	23.56	26.53
106.6	13.69	14.92	157.0	23.83	26.91
107.5	13.84	15.15	158.4	24.02	27.19
108.5	14.05	15.30	159.8	24.37	27.52
109.4	14.24	15.52	161.3	24.66	27.89
110.4	14.45	15.68	162.7	25.00	28.17
111.4	14.62	15.86	164.2	25.35	28.45
112.3	14.78	16.05	165.6	25.61	28.80
113.3	14.97	16.25	167.0	25.91	29.08
114.2	15.18	16.43	168.5	26.27	29.43
115.2	15.39	16.64	169.9	26.54	29.80
116.2	15.54	16.81	171.4	26.90	30.08
117.1	15.73	16.99	172.8	27.25	30.38
118.1	15.93	17.17	174.2	27.53	30.77
119.0	16.12	17.36	175.7	27.82	30.93
120.0	16.30	17.58	177.1	28.19	31.21
121.0	16.49	17.75	178.6	28.38	31.50
121.9	16.70	17.89	180.0	28.69	31.89
122.9	16.89	18.11	181.4	28.98	32.16
123.8	17.09	18.32	182.9	29.38	32.55
124.8	17.24	18.50	184.3	29.65	32.74
125.8	17.47	18.64	185.8	30.00	33.02
126.7	17.67	18.87	187.2	30.22	33.42
127.7	17.82	19.04	188.6	30.52	33.80
128.6	18.01	19.21	190.1	30.89	34.09
129.6	18.25	19.39	191.5	31.30	34.19
130.6	18.38	19.60	193.0	31.63	34.58
131.5	18.64	19.80	194.4	31.73	34.97
132.5	18.78	19.94	195.8	32.08	35.28

continued...

Table A.30 continued.

12 min run			30 min run		
Shear Stress (Pa)	Shear rate (s^{-1}) asc	dsc	Shear Stress (Pa)	Shear rate (s^{-1}) asc	dsc
133.4	19.01	20.17	197.3	32.52	35.46
134.4	19.15	20.32	198.7	32.84	35.87
135.4	19.40	20.54	200.2	33.02	36.16
136.3	19.58	20.71	201.6	33.46	36.46
137.3	19.81	20.86	203.0	33.73	36.77
138.2	19.98	21.08	204.5	34.05	37.05
139.2	20.16	21.28	205.9	34.38	37.35
140.2	20.37	21.40	207.4	34.66	37.69
141.1	20.59	21.60	208.8	35.02	37.98
142.1	20.76	21.81	210.2	35.33	38.25
143.0	20.94	21.96	211.7	35.67	38.48
144.0	21.22	22.17	213.1	35.91	38.90
145.0	21.35	22.38	214.6	36.24	39.19
145.9	21.57	22.62	216.0	36.61	39.40
146.9	21.79	22.85	217.4	36.94	39.80
147.8	21.97	23.01	218.9	37.20	40.11
148.8	22.19	23.20	220.3	37.59	40.30
149.8	22.37	23.34	221.8	37.95	40.72
150.7	22.55	23.60	223.2	38.19	41.16
151.7	22.75	23.91	224.6	38.61	41.24
152.6	22.96	24.27	226.1	38.95	41.54
153.6	23.16	24.59	227.5	39.20	41.76
154.6	23.32	24.70	229.0	39.54	42.06
155.5	23.59	24.88	230.4	39.77	42.37
156.5	23.73	25.04	231.8	40.09	42.69
157.4	23.89	25.16	233.3	40.42	43.01
158.4	24.06	25.41	234.7	40.75	43.35
159.4	24.27	25.70	236.2	41.12	43.67
160.3	24.50	25.84	237.6	41.46	44.00
161.3	24.77	25.92	239.0	41.82	44.18
162.2	24.95	26.14	240.5	42.15	44.57
163.2	25.08	26.43	241.9	42.42	44.81
164.2	25.32	26.64	243.4	42.87	45.17
165.1	25.56	26.72	244.8	43.12	45.37
166.1	25.85	26.89	246.2	43.49	45.76

continued...

Table A.30 continued.

12 min run			30 min run		
Shear Stress (Pa)	Shear rate (s^{-1}) asc	dsc	Shear Stress (Pa)	Shear rate (s^{-1}) asc	dsc
167.0	25.93	27.15	247.7	43.73	45.87
168.0	26.14	27.40	249.1	44.19	46.31
169.0	26.40	27.46	250.6	44.34	46.52
169.9	26.66	27.61	252.0	44.82	46.83
170.9	26.77	27.91	253.4	45.08	47.15
171.8	26.93	28.16	254.9	45.43	47.53
172.8	27.24	28.29	256.3	45.81	47.79
173.8	27.51	28.34	257.8	46.17	48.05
174.7	27.68	28.62	259.2	46.53	48.32
175.7	27.80	28.66	260.6	46.82	48.66
176.6	28.08	28.88	262.1	47.17	48.76
177.6	28.09	29.14	263.5	47.53	49.23
178.6	28.38	29.39	265.0	47.72	49.33
179.5	28.66	29.48	266.4	48.09	49.75
180.5	28.93	29.63	267.8	48.40	49.93
181.4	29.02	29.88	269.3	48.79	50.38
182.4	29.23	30.15	270.7	49.11	50.57
183.4	29.50	30.19	272.2	49.55	50.85
184.3	29.77	30.36	273.6	49.84	51.22
185.3	29.88	30.52	275.0	50.19	51.34
186.2	30.10	30.60	276.5	50.59	51.77
187.2	30.32	30.89	277.9	50.63	51.86
188.2	30.42	31.14	279.4	51.26	52.30
189.1	30.72	31.32	280.8	51.56	52.53
190.1	30.95	31.49	282.2	51.82	52.92
191.0	31.18	31.65	283.7	52.14	53.15
192.0	31.37	31.61	285.1	52.73	53.14
			286.6	52.93	53.63
			288.0	53.00	53.64

Table A.31: Peak torque values for chocolate samples at 40°C using different sized vanes with the Brabender Rheotron viscometer with the A cup and spring A.

Sample	Speed (rpm)	Peak Torque on Vane (Nm x 10^{-3})				
		E	F	G	K	O
HMC	0.064	0.4971	0.8925	1.420	1.959	2.231
	0.120	0.5224	0.9633	1.431	2.050	2.304
	0.224	0.5315	0.9578	1.508	2.014	2.395
HSS	0.064	0.6313	1.045	1.747	2.395	3.447
	0.120	0.6803	1.083	1.839	2.467	3.410
	0.224	0.7075	1.148	1.916	2.485	3.664
H1	0.064	1.121	3.193	3.229	4.136	4.698
	0.120	1.094	3.138	3.102	4.063	4.880
	0.224	1.143	3.193	3.175	4.316	5.007
H2	0.064	0.4608	0.8653	1.148	2.014	2.413
	0.120	0.4916	0.9143	1.442	2.249	2.449
	0.224	0.5079	0.9415	1.502	2.213	2.685